Self-consistent-field modeling of complex molecules with united atom detail in inhomogeneous systems. Cyclic and branched foreign molecules in dimyristoylphosphatidylcholine membranes

L. A. Meijer, F. A. M. Leermakers, and J. Lyklema

Citation: J. Chem. Phys. **110**, 6560 (1999); doi: 10.1063/1.478562
View online: http://dx.doi.org/10.1063/1.478562
View Table of Contents: http://jcp.aip.org/resource/1/JCPSA6/v110/i13
Published by the American Institute of Physics.

Self-consistent-field modeling of complex molecules with united atom detail in inhomogeneous systems. Cyclic and branched foreign molecules in dimyristoylphosphatidylcholine membranes

L. A. Meijer, F. A. M. Leermakers,[a] and J. Lyklema
Laboratory of Physical Chemistry and Colloid Science, Wageningen Agricultural University, Dreijenplein 6, 6703 HB Wageningen, The Netherlands

(Received 6 April 1998; accepted 6 January 1999)

We have developed a detailed self-consistent-field model for studying complex molecules in inhomogeneous systems, in which all the molecules are represented in a detailed united atom description. The theory is in the spirit of the approach developed by Scheutjens and co-workers for polymers at interfaces and self-assembly of surfactants and lipids into association colloids. It is applied to lipid membranes composed of dimyristoylphosphatidylcholine (DMPC). In particular, we looked at the incorporation of linear, branched, and cyclic molecules into the lipid bilayers being in the liquid phase. Detailed information on the properties of both the lipids and the additives is presented. For the classes of linear and branched alcohols and phenol derivatives we find good correspondence between calculated partition coefficients for DMPC membranes and experimental data on egg-yolk PC. The calculated partitioning of molecules of isomers, containing a benzene ring, two charged groups (one positive and one negative) and 16 hydrocarbon segments, into DMPC membranes showed variations of the partition coefficient by a factor of 10 depending on the molecular architecture. For zwitterionic additives we find that it is much more difficult to bring the positive charge into the membrane core than the negative one. This result can be rationalized from information on the electrostatic potential profile of the bare membrane, being positive in both the core and on the membrane surface but negative near the position of the phosphate groups. For several tetrahydroxy naftalenes we found that, although the partition coefficient is barely influenced, the average orientation and position of the molecule inside the membrane is strongly dependent on the distribution of the hydroxyl groups on the naphthalene rings. The orientation changes from one where the additive spans the membrane when the hydroxyls are positioned on (2,3,6,7) positions, to an orientation with the rings parallel to the membrane surface and located near the head group–hydrophobic core interface for the hydroxyls at the (1,3,5,7) positions. We propose that, when our model is used in combination with octanol/water partitioning data, a very accurate prediction is possible of the affinity of complex molecules for lipid membranes. [S0021-9606(99)51413-X]

I. INTRODUCTION

Biomembranes are composed of a large number of constituents.[1] Phospholipids are essential components of it. These molecules consist of a glycerol backbone onto which two apolar tails, 12 to 24 carbon atoms long, and a polar head group are attached. The head group contains a phosphate group esterified to the glycerol and often some other polar group like choline, ethanol amine, or glycerol. Stable model membranes are formed when one single type of lipid is added to water. For this reason it is attractive to start with such a highly simplified system to model membranes.[2]

The next step in the modeling of biomembranes is to study the effect of adding foreign molecules to the phospholipid matrix. By doing this, one can systematically study both the influence of the additives on the bilayer structure and the position, orientation, and partition of these molecules. One can consider various types of additives, such as other (phospho-)lipids, ions, or biologically active molecules, e.g., hormones or manmade drugs.

For the latter two classes of ''foreign'' molecules a parameter of special interest is the partition coefficient. This quantity is defined as the ratio between the concentration of a foreign molecule in the membrane phase and that in the water phase. The partitioning of the above-mentioned molecules in the membrane matrix is important because it plays a role in the working mechanism of the drug or hormone. For example, the passive transport through the membrane is obviously strongly dependent on this partition coefficient. If the working site of a drug is known, one can propose an optimal partition coefficient for such a drug. If one could predict partition coefficients from molecular details one would speed up the search for new drugs enormously. It is this ultimate goal that has motivated us to perform the present study.

Well-controlled experiments on lipid bilayer systems are certainly not easy and the interpretation of the data is facili-

[a]Electronic mail: frans@fenk.wau.nl

tated when good theories are available. In fact, the modeling *per se* is a useful alternative approach to obtain insight into the structure of lipid membranes. Theoretical modeling is nowadays possible with the help of fast computers.

Surprisingly little work has been done in recent years on the theoretical modeling of additives in lipid bilayer membranes. Due to the complexity of membranes, there is still much progress to be made on this subject. There are a few theoretical techniques that have been applied with reasonable success. Molecular dynamics (MD) simulations on the interactions between the lipid matrix and additives[3–6] are probably the most detailed, but are computationally extremely intensive. Significantly more coarse grained Monte Carlo (MC) simulations are due to Mouritsen *et al.*[7–9] Here the bilayer membrane is modeled as a two-dimensional sea in which the molecules can have several states. With state-dependent interactions they can calculate the lateral structure formation. There is, however, the difficulty of, *a priori*, determining the various states and corresponding interactions for a (new) molecule from its molecular structure.

An alternative theoretical modeling option applied to lipid membranes, and used in this paper, is known under the term self-consistent-field (SCF) theories. SCF methods are computationally inexpensive. The method is based on the reduction of the many-molecule problem to the problem of one molecule in the (external) field of mean force of all the others. In general, the external field is defined depending on the set of all conformations of all molecules and their interactions. The potential field, in its turn, determines the statistical weight of the conformations that make up the complete system. The fixed point solution of this implicit set of equations is referred to as the self-consistent-field solution, which typically depends on boundary conditions and space filling constraints.

Several groups have elaborated various approaches along these lines to describe the association of molecules into aggregates. Some authors make use of a type of lattice (not necessary matched to the segment size) to specify the symmetry of the aggregates, to specify the local values of the external fields and/or to enumerate the various possible conformations. In some cases one considers the aliphatic chains to be attached to the surface of the aggregate, but do not allow solvent (water) to penetrate into the aggregate. The external field is mostly a pressure field that ensures that the core of the aggregate has a density comparable to that of liquid alkane.[10–14] Sometimes an order-dependent field is introduced.[15,16] Marčelja showed that the gel to liquid phase transition could be generated in this way. Additives in bilayers are either modeled as structureless isotropic monomers that mostly have no specific contact interaction with the lipid tails, or small chain molecules of the same type of units as the tail segments. The results are, despite these approximations, promising and give insight into the importance of the included field components.

The theory discussed in this paper includes not only volume interactions and an anisotropic field (of a different origin than used by Marčelja or Gruen), it also includes electrostatic interactions and contact interactions between unlike segments in a Bragg–Williams approximation, parametrized by way of Flory–Huggins χ parameters. These interactions allow the lipids to self-assemble in a given geometry. Apart from the lattice geometry, nothing is assumed about the segment position or orientation.

Several years ago, simplified model membranes were investigated with this theory.[17–19] Although the molecular representation was rather crude, the main features of the tail region, i.e., the large degree of disorder and the fact that the segments closest to the hydrophobic–hydrophilic ''interface'' in the lipid molecules have the most narrow distribution, were reproduced, in line with MD predictions. In order to relate to experiments, calculations were done on adsorbed phospholipid monolayers with a more realistic molecular description.[20] It was found that the zwitterionic nature of DMPC gives rise to a profile in the electrostatic potential, which, in turn, causes cations to associate with the phosphate group. The association is stronger, the higher is the valence of the ions. These results were of interest in interpreting the ion permeability measurements of monolayers deposited on a mercury electrode, and used to conjecture that the concentration of ions in the head group area is a determining factor for their permeability through ion channels.[21,22]

More recently, we considered the head group conformations of (modified) DMPC and DMPS membranes.[23] The PC head group appeared to have, on average, a conformation parallel to the membrane surface. In line with experimental data,[24] it was found that, at high salt concentrations, the choline group distribution splits in two orientations: one closer to the hydrocarbon phase and the other closer to the water phase.

Despite these promising results, several shortcomings of our theory remain that deserve further attention. One of these is that, up to date, only flexible linear or branched molecules could be considered. Most biologically active additives to membranes have, however, some sort of rigid (ring) moiety as a part of their structure. Membranes are highly ordered systems (although not as high as some pictorial representations seem to imply), and thus a considerable difference in packing behavior is expected between flexible and rigid species in the membrane. Furthermore, the position of different types of substituents on a ring structure is likely to be significant for, e.g., the partitioning.

In the following we will discuss in detail a SCF framework to handle complex molecules with atomic detail in inhomogeneous systems. First we will present the partition function for the system. Next we will discuss the propagator method to obtain the density profiles for flexible and branched chain molecules using a Rotational Isomeric State (RIS) scheme. We proceed by giving the details of the treatment of rigid structures within this propagator formalism. This extension is the central topic of this paper. Results will be presented for the partition coefficients of linear and branched alcohols and phenols in DMPC membranes. The positional and orientational information of additives in DMPC membranes will be shown for a group of isomers containing a benzene ring with some substituents and of some, in various ways substituted, tetrahydroxy naftalenes.

Finally, we will discuss the perspectives of our approach and present our conclusions.

II. THEORY

A. Preliminary considerations

In a SCF theory the full membrane problem is reduced to one test molecule (i.e., lipid or additive) in the potential field of mean force of all the other molecules. The problem splits naturally into two: how to relate the potential fields to the densities and to relate the densities to the potential fields. Both subproblems can be tackled from the approximate partition function for the system. This quantity has been derived before and can be applied to the present system as well. Here the highlights of the derivation will be briefly reviewed and proper notations are introduced. We start by introducing the parameters and key approximations.

The partition function is the sum over the probabilities of all sets of all conformations of all molecules in the system. To compute this properly, several quantities have to be defined. Molecules of different types (water, lipid, salt, additive) are numbered $i=1,2,\ldots$. Each molecule of type i consists of N_i units (segments). Each unit represents an atom or a group of atoms (e.g., CH_2 or OH). We use $A,B,\ldots$, to denote the types of segments. The segments in the molecule are referred to by ranking numbers $1,2,\ldots,s_i,\ldots,N_i$ and linked to each other by bonds, which, in turn, are numbered $1,2,\ldots,\sigma_i,\ldots,N_{\sigma i}$, where $N_{\sigma i}$ denotes the number of bonds of molecule i. In linear or branched chains $N_{\sigma i}$ is one less than the number of segments N_i. If ring fragments are part of the molecule, $N_{\sigma i}$ increases by one for every closed ring in the structure. A conformation, c, is defined by the position in space of one segment (e.g., the first segment of the chain) and the subsequent orientation of all bonds in the molecule. Note that every configuration is L-fold degenerated, because every first segment in a chain can occupy one of the L sites in layer z.

In order to keep the full set of all conformations, $\{n_i^c\}$, from becoming infinite, the system volume is discretized. A system of coordinates with spacings l spans up a lattice in which flat layers are identified that accommodate L sites of equal volume l^3 each. The layers are numbered $1,2,\ldots,z,\ldots,M$, with M being the total number of layers. All segments are assumed to fit exactly a lattice site. Within each layer a mean-field approximation is applied as only the average occupation is recorded. The number of directions of the bonds is also limited: only four distinct directions are allowed for. A tetrahedral lattice is applied on which a three-choice propagation scheme is employed. This three-dimensional lattice can be mapped onto a two-dimensional square lattice, which is shown in Fig. 1. In this two-dimensional representation the four bond directions e, f, g, and h are indicated as vectors connecting segments in between layers z and $z-1$ (e), within a layer z (f and g) and between layer z and $z+1$ (h).

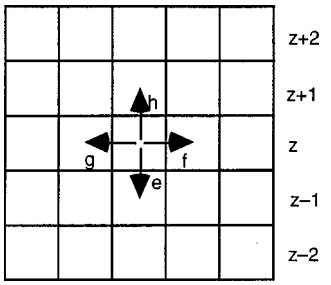

FIG. 1. A two-dimensional square lattice representation of the tetrahedral (diamond) lattice used in this paper with the four directions indicated (e, f, g, and h).

By the introduction of a lattice, not only is the counting of the conformations simplified, but also the geometry of the system, the length of the bonds, and the size of the segments are fixed. These approximations can be relaxed in various ways. One way to do this is to reduce the lattice spacing while keeping the segment volume constant.[25] The assumption of a fixed bond length can be partly relaxed by allowing certain fragments with different bond lengths (like rigid rings) to have their segments on off-lattice sites. However, after the sampling of the conformations one needs to assign the segment to the layers and the bonds to one of the set of directions $\{e,f,g,h\}$.

To give every conformation the proper statistical weight, the energy of each conformation in the external field is determined. For a molecule in a given conformation every segment has a known z position. Depending on the segment type A of a unit, it feels the local segment potential energy, $u_A(z)$. The total potential energy of the molecule in that conformation is then found by the sum of the segment potential energies of all segments. Then the overall probabilities to find the segments of molecule i in conformation c on their respective positions is related to the potential energy by a Boltzmann weighting factor. Directly linked to this probability is the number of molecules i in conformation c. This quantity is referred to by n_i^c.

The number of molecules i in conformations c follows the partition function that is maximized with respect to every n_i^c. If n_i^c is known, the approximate (mean field) partition function is available. From this all thermodynamic properties follow.

B. The partition function

Formally the grand canonical partition function for an open system, $\Xi(\{\mu_i\},M,L,T)$, can be written as

$$\Xi(\{\mu_i\},M,L,T)=\Xi^*\frac{\Sigma_{\{n_i^c\}}\Omega(\{n_i^c\})Q^{\sigma}\exp(U^{\mathrm{int}}/k_{\mathrm{B}}T)\exp(\Sigma_i n_i\mu_i/k_{\mathrm{B}}T)}{\Sigma_{\{n_i^c\}}\Pi_i\Omega_i^*(n_i)Q^{\sigma *}\exp(U^{\mathrm{int}*}/k_{\mathrm{B}}T)\exp(\Sigma_i n_i\mu_i^*/k_{\mathrm{B}}T)}. \tag{1}$$

It is composed of a combinatorial factor Ω, an internal canonical partition function Q^{σ}, which takes the local bond configurations into account, the interaction energy U^{int} and the chemical potentials $\{\mu_i\}$. The corresponding reference states for every molecule (here we choose these to be the one component amorphous melts) are indicated by an asterisk. The absolute temperature is denoted by T and Boltzmann's constant by k_{B}.

The interaction energy U^{int} is split into two contributions with respect to the amorphous reference state of pure molecule i. One is of short range and extends over three consecutive layers. It is parametrized by the Flory–Huggins χ parameter. The interaction parameter χ_{AB} is the dimensionless-free energy involved in the exchange of a segment of type A from a pure A solution with a segment B from a pure B solution. So it is zero by definition for the exchange of segments of the same type. The other part of the interaction energy is (especially at low ionic strength) of long range, extending over the whole system, and is of electrostatic origin. It contains the electrostatic potential $\Psi(z)$ that can be calculated, through Gauß' law, from the density profile, involving the dielectric permittivity profile, $\epsilon_r(z)$, and the charge (valence) profile, $q(z)=\Sigma_A e\nu_A\varphi_A(z)$.[23,26,27] In this last equation ν_A is the valence of segment A, $\varphi_A(z)$ the volume fraction of that segment at position z, and e the elementary charge. The potential in the reference state is taken to be zero. The total interaction energy then reads as

$$\frac{U^{\text{int}}-U^{\text{int}*}}{k_{\text{B}}T}=\frac{1}{2}\sum_i\sum_z\sum_A\sum_B N_{Ai}(z)\chi_{AB}[\langle\varphi_B(z)\rangle-\varphi_{Bi}^{*}]+\sum_z\frac{Lq(z)\Psi(z)}{2k_{\text{B}}T}. \tag{2}$$

In Eq. (2), $N_{Ai}(z)$ is the number of segments of type A that molecule i has in layer z. The angular brackets denote the averaging over three consecutive layers: $\langle\varphi_B(z)\rangle=\frac{1}{3}\varphi_B(z-1)+\frac{1}{3}\varphi_B(z)+\frac{1}{3}\varphi_B(z+1)\approx\varphi_B(z)+\frac{1}{3}[\partial^2\varphi_B(z)/\partial z^2]$.

The internal canonical partition function, Q^{σ}, takes into account the energetic and entropic contributions that the various conformations of a bond sequence can have. In this term only contributions of intramolecular interaction that are not accounted for in the (external) potential fields are included. More specifically in a linear chain, it is the energy and entropy involved with the different *gauche* and *trans* conformations along the chain. In general, the local conformations (*gauche* and *trans*) are defined by the relative directions of the bonds in the immediate vicinity of one bond σ. It is assumed that the conformation of the rest of the chain does not influence the energy concerned with this ''local conformation.'' The local conformation around bond σ is denoted by $q_{\sigma i}$ and the energy of a specific conformation as $u^{q_{\sigma i}}$. For a given conformation c of a molecule, the local conformation around bond σ is denoted by $q_{\sigma i}^{c}$. So the conformation c of the full chain can be determined by the local conformations $\{q_{\sigma i}^{c}\}_{\sigma}$.

As an example, in a linear hydrocarbon chain $q_{\sigma i}$ for $1<\sigma<N_{\sigma i}$ determines the relative directions of three consecutive bonds and therefore the relative positions of four consecutive segments. Such a fragment can have three local conformations: one *trans* and two *gauche* ones. In contrast to the two *gauche* ones, in the *trans* conformation the two bonds $\sigma-1$ and $\sigma+1$ are pointing in the same direction. By rotation around the central bond σ the bond sequence can assume these local states (see Fig. 2). We denote the energy difference for the rotation from *gauche* to *trans* of the conformation $q_{\sigma i}$ as u^{g_σ}. We note that u^{g_σ} can vary along the chain.

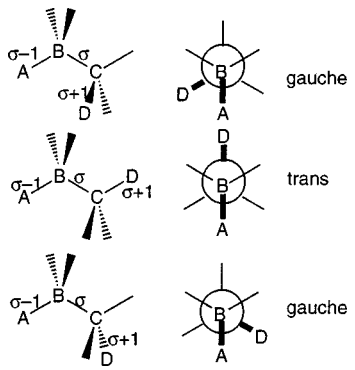

FIG. 2. An illustration of the three possible local bond conformations in a linear chain. The central bond is denoted as σ, and A, B, C, and D are four consecutive segments. Other segments in the chain are not shown.

The probability, $\lambda^{q_{\sigma i}}$, for a specific local conformation $q_{\sigma i}$ is related to the Boltzmann factor, containing the internal energy $\lambda^{q_{\sigma i}}$. The proper normalization is found by the sum of the Boltzmann factors of all possible local conformations around that bond σ, $\{q'_{\sigma i}\}$:

$$\lambda^{q_{\sigma i}}=\exp(-u^{q_{\sigma i}}/k_{\text{B}}T)\Big/\sum_{q'_{\sigma i}}\exp(-u^{q'_{\sigma i}}/k_{\text{B}}T). \tag{3}$$

For a linear chain part the probability to find a *gauche* conformation around bond σ then becomes $\lambda^{q_{\sigma i}}=\lambda^{q_\sigma}=\exp(-u^{g_\sigma}/k_{\text{B}}T)/[2\exp(-u^{g_\sigma}/k_{\text{B}}T)+1]=1/[2+\exp(u^{g_\sigma}/k_{\text{B}}T)]$. The probability to find a *trans* conformation is simply $\lambda^{t_\sigma}=1-2\lambda^{g_\sigma}$. At the chain ends ($\sigma=1$ and $\sigma=N_{\sigma i}$, respectively, for linear chains) there is only one neighboring bond ($\sigma=2$ and $\sigma=N_{\sigma i}-1$, respectively). Since all bonds have the same angles in a tetrahedral lattice, only one conformation exists which, according to Eq. 3, has a probability of unity.

In a branched chain there are more then two end bonds σ for which $\lambda^{q_{\sigma i}}=1$. Moreover, local conformations including a branch point have a specific problem. We have chosen in this article not to differentiate between occupancies between the f and g directions (the isotropic distribution of bonds in a plane). Consequently, our calculations always represent racemic mixtures. As a result of this, the number of local conformations including a branch point equals six [see Fig. 3(a)]. Let the branch point be defined by the three bonds σ, σ', and σ'' that come together. We focus on bond σ, which has, besides σ' and σ'', also σ° as a neighbouring bond. These four bonds (five segments) form the relevant fragment with conformations $\{q_{\sigma i}\}$. These conformations can be grouped into two sets according to their internal energy: one set for two *gauche–gauche* conformations with a higher energy and one set of four *trans–gauche* conformations with a

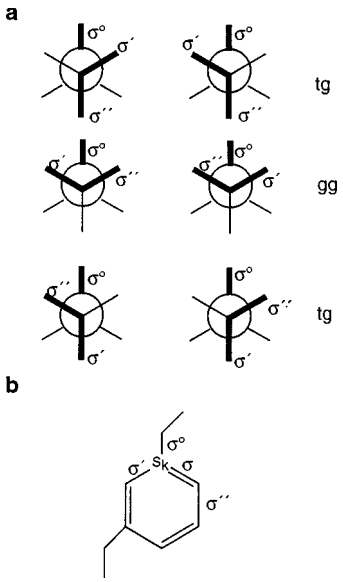

FIG. 3. Diagram (a) presents the six possible local conformations close to a branch point with three bonds (three node). There are four separate *trans–gauche* (tg) and two gauche–gauche (gg) conformations. Diagram (b) shows the only possible local bond conformation around a bond σ in a benzene ring. Here bond σ° is the ''outgoing'' bond on segment s_k.

lower energy. In calculating the probability for a specific *gauche–gauche* conformation, only the energy difference u^{gg_σ} is needed: $\lambda^{q_{\sigma i}}=\exp(-u^{gg_\sigma}/k_BT)/[2\exp(-u^{gg_\sigma}/k_BT)+4]=1/[2+4\exp(u^{gg_\sigma}/k_BT)]=\lambda^{gg_\sigma}$. The probability to find a *trans–gauche* conformation then is simply $\lambda^{tg_\sigma}=\frac{1}{4}-\frac{1}{2}\lambda^{gg_\sigma}$.

A similar way of reasoning applies for a segment (node) where four branches come together (four node). In this case five bonds and six segments are involved in the relevant fragment with conformations $\{q_{\sigma i}\}$. Now no energetic difference is made between the three bonds on the branch point $(\sigma',\sigma'',\sigma''')$ next to bond σ. So the same internal energy is assigned to all viable conformations of these five bonds. Therefore, the probability for each of the six local conformations is equal to $\lambda^{q_{\sigma i}}=\frac{1}{6}$. Again, to simplify the calculations, here too an isotropic occupancy of the *f* and *g* directions is imposed. This has the result that molecules with a branch point with four connecting bonds are calculated as racemic mixtures. Equation (3) can also be applied to bonds in rigid fragments [see Fig. 3(b)]. In these fragments there is obviously only one local conformation allowed and thus the denominator of Eq. (3) extends over just this one conformation and, consequently, $\lambda^{q_{\sigma i}}=1$ for all bonds inside the rigid unit.

We have now specified the local probability factor that is assigned [with Eq. (3)] to each bond in the (complex) molecules. The product of these probabilities over all bonds for a molecule *i* in a given conformation *c* can be evaluated, and this quantity is subsumed in $Q^{\sigma}/Q^{\sigma *}$. For a trimer, the unnormalized contribution to this part of the partition function is unity. The two bonds have only one local conformation each. Taking into account the rotational freedom of the whole molecule, a normalization constant, $\lambda^{\alpha\beta}$, is found. Such a trimer can have $3Z$ conformations, where Z represents the number of different bond directions: the first bond has Z directions to choose from and the second than has only three alternatives left. In the same way molecules with more bonds also have $3Z$ degrees of rotational freedom. The natural logarithm of the internal canonical partition function with respect to the reference state now reads as

$$\ln\left(\frac{Q^{\sigma}}{Q^{\sigma *}}\right)=\sum_i\sum_c n_i^c\ln\left(\frac{1}{3Z}\prod_{\sigma}\frac{\exp(-u^{q_{\sigma i}^c}/k_BT)}{[\Sigma_{q_{\sigma i}}\exp(-u^{q_{\sigma i}}/k_BT)]}\right)$$

$$=\sum_i\sum_c n_i^c\ln\left(\lambda^{\alpha\beta}\prod_{\sigma}\lambda^{q_{\sigma i}^c}\right). \tag{4}$$

Next, the term Ω in the partition function Ξ will be discussed. This quantity has been derived by Leermakers and Scheutjens.[19] Their result also applies to our system, even when we adopt complex-shaped molecules:

$$\ln(\Omega/\Omega^*)=-\sum_i\sum_c n_i^c\ln\frac{n_i^cN_i}{L}+\frac{L}{2}$$

$$\times\sum_z\sum_{\alpha''}[1-\varphi^{\alpha''}(z|z')]\ln[1-\varphi^{\alpha''}(z|z')]$$

$$-ML\sum_i\sum_{\alpha''}(\varphi_i-\varphi_i^{\alpha''*})\ln(1-\varphi_i^{\alpha''*}). \tag{5}$$

In this equation, $\varphi^{\alpha''}(z|z')$ is the fraction of maximum bond density possible in orientation α'' starting in layer z and ending in layer z' (cf. Fig. 1 and Table I). Below we use $\varphi^{\alpha''b}$, which is the fraction of possible bonds in orientation α'' in the bulk defined as $\varphi^{\alpha''b}=[Z\Sigma_i\varphi_i^b(N_{\sigma i}/N_i)]^{-1}$.

The factor Ω takes into account the number of ways the set of all the conformations $\{n_i^c\}$ can be put into the system. Here, not only the random mixing of the conformations, provided every layer is filled with L segments, is considered, but, in addition, the entropy of placing bonds in the lattice is included. It was recognized by DiMarzio that parallel bonds located at the same z coordinate cannot block each other.[28,29] This notion enables one to rather accurately calculate the vacancy probability needed for the packing of the chains in the lattice. In effect, an anisotropic field is created that has the property that, when it is large (due to the fact that many bonds have a given orientation), it will force other bonds to assume this orientation too. This cooperative behavior is responsible for the gel-to-liquid phase transition in bilayer membranes.[19] The two terms in Eq. (5) that depend on α'' are the result of this anisotropic weighting of the bonds in the lattice.

We note that in Eq. (5) the bond orientations α'' are limited to the primary orientations e'', f'', g'', and h'', as

TABLE I. Collection of the direction α and the connecting direction α' combined with the relations of α to z'.

α (layer z)	α' (layer z')	z'
e	h	$z-1$
f	g	z
g	f	z
h	e	$z+1$

indicated by Fig. 1. The following procedure is adopted to place rigid structures in the system. If such a fragment of a molecule contains units that do not exactly fit onto the lattice layers, a representative set of conformations is sampled (see the Appendix). A segment in a fragment that is in a given conformation feels the external potential field of the layer in which the center of that unit resides. In this procedure the bonds in the ring can have other orientations than defined by $\alpha'' \in \{e,f,g,h,e',f',g',h'\}$. We use the ansatz that these bonds are assigned to the bond orientation α'' that is closest to the direction of the bond of interest. More details will be given below.

We return once more to Eq. (1): The chemical potentials μ_i still need to be discussed. In an equilibrated system, the chemical potentials do not depend on the spatial coordinate. In the bulk phase, denoted with the superscript *b*, no gradients in the densities occur, which facilitates the computation of these quantities. The chemical potential can be derived from the canonical partition function for a homogeneous system and written as a function of bulk values and reference state values only.[19] Here we have a slightly modified version, which is correct even when the molecules contain closed rings or another exotic internal structure (see the Appendix),

$$\frac{\mu_i-\mu_i^*}{kT}=\ln\varphi_i^b-\frac{N_i}{2}\sum_A\sum_B(\varphi_{Ai}^*-\varphi_A^b)\chi_{AB}(\varphi_{Bi}^*-\varphi_B^b)-(ZN_i-N_{\sigma i})\ln\left(1+\frac{N_{\sigma i}-N_i\Sigma_j\frac{N_{\sigma j}\varphi_j^b}{N_j}}{ZN_i-N_{\sigma i}}\right). \tag{6}$$

The first term, $\ln\varphi_i^b$, is the ideal mixing term with φ_i^b the volume fraction of molecule *i* in the bulk phase. The second term in Eq. (6) accounts for the contact interactions between unequal segment of types *A* and *B* with respect to the reference state of a melt of pure molecules of type *i*, denoted by the asterisk. The last term in Eq. (6) is the modified Flory–Huggins mixing term, which takes inter- and intramolecular correlations between bonds into account. The bond correlations that are included in the present theory account for the fact that a step in a certain direction cannot be blocked by one of the segments on bonds in the same direction.

To find the equilibrium set of conformations of the molecules in the system, under the constraint that all lattice layers are exactly filled $[\Sigma_i\varphi_i(z)=1]$, we introduce Lagrange multipliers $u''(z)$ to define the unconstrained function *f*:

$$f=k_BT\ln(\Omega/\Omega^*)+k_BT\ln(Q^\sigma/Q^{\sigma*})-(U^{\rm int}-U^{\rm int*})+\sum_i n_i(\mu_i-\mu_i^*)+\sum_z u''(z)\left(L-\sum_i\sum_c n_i^cN_i^c(z)\right). \tag{7}$$

Now, in the equilibrium distribution of the set of conformations, the derivative $\partial f/\partial n_i^c$ equals zero for every conformation n_i^c. After some straightforward mathematics we find that the equilibrium number of molecules *i* in conformation *c* in the system can conveniently be expressed by

$$n_i^c=LC_i\lambda^{\alpha\beta}\prod_{s=1}^{N_i}G_i^c(z,s)\prod_{\sigma=1}^{N_{\sigma i}}[\lambda^{q_{\sigma i}^c}G_i^c(z,\sigma)], \tag{8}$$

where $G_i^c(z,s)$ is the free segment weighting factor for segment *s* of molecule *i* in layer *z*. The superscript *c* fixes the *z* coordinates for all the segments and the directions of the bonds. This free segment weighting factor is given by the Boltzmann factor of the potential energy field $u(z)$ and, if segment *s* of molecule *i* is of type *A*, is given by

$$G_A(z)=\exp\left(-\frac{u'(z)}{k_BT}-\sum_B\chi_{AB}\langle\varphi_B(z)-\varphi_B^b\rangle-\frac{\nu_Ae\Psi(z)}{k_BT}\right), \tag{9}$$

where $u'(z)=u''(z)-u''^b$, so that the segment weighting factor is properly normalized to unity in the bulk. We return below to the consequences of the fact that $G_A(z)=1$ in the bulk. The Lagrange parameter in the bulk u''^b reads as

$$u''^b/k_BT=-1-\sum_{\alpha''}\ln(1-\varphi^{\alpha''b})-\frac{1}{2}\sum_A\sum_B\chi_{AB}\varphi_A^b\varphi_B^b. \tag{10}$$

The $u'(z)$ term in Eq. (9) does not depend on the segment type. It can be regarded as a hard core potential that takes excluded volume effects into account, since it arises from the Lagrange multipliers that satisfy the constraint that each layer of *L* lattice sites is exactly filled with *L* segments. The last factors in Eq. (8), $G_i^c(z,s)$, are the anisotropic bond weighting factors arising from the combinatorial factor Ω. They depend on the orientation (direction) of the bond σ. If this bond starts in layer *z* and ends in layer z' (having direction α'' in conformation *c*), it is given by

$$G_i^c(z,\sigma)=G^{\alpha''}(z|z')=\frac{1-\varphi^{\alpha''b}}{1-\varphi^{\alpha''}(z|z')}. \tag{11}$$

Next, the normalization constant C_i needs to be defined. For an open system where we use the grand canonical partition function, it is

$$C_i=\frac{\varphi_i^b}{N_i}, \tag{12}$$

and in this case the number of molecules of type *i* in the system is fixed, i.e., a closed system where we use the canonical partition function, it is

$$C_i=\frac{\theta_i}{N_iG_i(N_{i1})}. \tag{13}$$

In this equation, $G_i(N_{i1})=\Sigma_c\lambda^{\alpha\beta}\Pi_sG_i^c(z,s)\Pi_\sigma[\lambda^{q_{\sigma i}^c}\times G_i^c(z,\sigma)]$ is the total weighting factor per lattice site of all the molecules of type *i* in the system and $\theta_i=\Sigma_z\varphi_i(z)$

$=\Sigma_c n_i^c N_i/L$ is the total amount of molecule i per lattice site. Below, a more convenient expression for $G_i(N_{i1})$ will be given.

C. The chain propagation scheme

The probability for a given chain to be in a specified conformation is usually not really an interesting quantity to know. More interesting are the density profiles $\{\varphi\}$ that result from the whole set of conformations $\{n_i^c\}$. As the partition function discussed above can also be written in terms of volume fraction profiles,[30] it is attractive to use methods that sum directly over the complete set of conformations. There are efficient propagator methods available to find the density profiles if one accepts the use of a Markov approximation. In this paper a special version known as the rotational isomeric state (RIS) scheme is used. In this scheme a bond can have four separate orientations within the lattice: $\alpha''=e''$, f'', g'' or h'' (see Fig. 1 and Table I). In each orientation α'' we distinguish two directions, α' and α. The direction e denotes the direction from one layer, z, to the previous one, $z-1$; f and g denote the two separate directions within a layer and h denotes the direction from one layer, z, to the next one, $z+1$ (cf. Fig. 1). The bonds *on* a segment are numbered σ_1 and σ_2 with the first bond, σ_1, pointing to the neighboring segment with the lower ranking number and the second one, σ_2, to the neighboring segment with a higher ranking number. Below we use the notation s_{12}, where the ''1'' denotes σ_1 and the ''2'' σ_2. The volume fraction of a segment s of molecule i with σ_1 in direction α and σ_2 in direction β is the sum over all conformations c with segment s in layer z and the bonds in these directions of the number of molecules in such conformations. Defining $q_i^c(z,s_{12}^{\alpha\beta})=1$ when the molecule in conformation c has segment s in layer z with its bonds 1,2 in the indicated directions α,β, respectively, and zero otherwise we may write

$$\sum_c \frac{q_i^c(z,s_{12}^{\alpha\beta})n_i^c}{L} = \varphi_i(z,s_{12}^{\alpha\beta}) = C_i\lambda^{\alpha\beta}\frac{G_i(z,s_1^{\alpha\beta})G_i(z,s_2^{\alpha\beta})}{G_i(z,s)}. \tag{14}$$

In Eq. (14) the free segment weighting factor $G_i(z,s)=G_A(z)$ if segment s in molecule i is of type A, which is defined as in Eq. (9). The subscripts 1 and 2 on the segment number s denote if either σ_1, or σ_2, or both σ_1 and σ_2 are connected to the rest of the chain. The end segment weighting factors $G_i(z,s_1^{\alpha\beta})$ and $G_i(z,s_2^{\alpha\beta})$ are defined recursively as follows:

$$G_i(z,s_1^{\alpha\beta}) = \sum_{\gamma'} [G_i(z',s_1'^{\gamma'\alpha'})\lambda_{\sigma i}^{\gamma''-\alpha''-\beta''}] \times G^{\alpha''}(z|z')G_i(z,s), \quad s>2, \tag{15a}$$

$$G_i(z,s_2^{\alpha\beta}) = G_i(z,s)G^{\beta''}(z|z')\sum_{\gamma'} [\lambda_{\sigma i}^{\alpha''-\beta''-\gamma''} \times G_i(z',s_2'^{\beta'\gamma'})], \quad s<N_i-1. \tag{15b}$$

The z' refers to z, $z-1$, or $z+1$, depending on the bond direction (see Table I), the prime on the segment number s indicates that the ranking number of a segment next to segment s defined by the chain architecture should be used. In a linear chain this is $s-1$ for the preceding and $s+1$ for the following segment. The $\lambda_{\sigma i}^{\alpha''-\beta''-\gamma''}$ in Eq. (15) is the same as $\lambda^{q_{\sigma i}}$ in Eq. (3), with the local bond conformation $q_{\sigma i}$ written specifically as the three consecutive bond directions $\alpha''-\beta''-\gamma''$. If γ'' equals α'', the three bonds have a *trans* configuration and $\lambda_{\sigma i}^{\alpha''-\beta''-\gamma''}$ can be written as $\lambda^{t_{\sigma i}}$. Direct back-folding is excluded because if either γ'' or α'' equals β'', $\lambda_{\sigma i}^{\alpha''-\beta''-\gamma''}\equiv 0$. When $\alpha''\neq\gamma''$ and $\alpha''\neq\beta''$ and $\gamma''\neq\beta''$ the configuration is *gauche*, and $\lambda_{\sigma i}^{\alpha''-\beta''-\gamma''}$ can be written as $\lambda^{g_{\sigma i}}$. Applying the relations of Eq. (15) recursively all end segment probabilities of the full chain can be calculated and from these the volume fraction profile follows using Eq. (14). The scheme is started by realizing

$$\begin{aligned} G_i(z,2_1^{\alpha\beta}) &= G_i(z',1)G^{\alpha''}(z|z')G_i(z,2), \\ G_i(z,[N_i-1]_2^{\alpha\beta}) &= G_i(z,N_i-1)G^{\beta''}(z|z')G_i(z',N_i). \end{aligned} \tag{16}$$

The overall statistical weight to find a chain in the system [cf. Eq. (13)] can now be calculated as $G_i(N_{i_1})=\Sigma_\alpha\Sigma_z G_i(z,N_{i1}^\alpha)$.

The fraction of maximum bond density for bond σ in molecule i, $\varphi_{\sigma i}^{\alpha''}(z|z')$, is calculated by the summation of the volume fractions over all appropriate orientations of the segments on both ends of the bond. The total fraction of maximum bond density as used in Eqs. (5) and (11) is then calculated by summation over the contributions of all bonds of all molecules:

$$\begin{aligned} \varphi^{\alpha''}(z|z') &= \sum_i \sum_\sigma \varphi_{\sigma i}^{\alpha''}(z|z') \\ &= \frac{1}{2}\sum_i \left\{ \sum_{s=2}^{N_i-1} \sum_{\beta''} [\varphi_i(z,s_{12}^{\alpha\beta}) + \varphi_i(z',s_{12}^{\alpha'\beta'}) + \varphi_i(z,s_{12}^{\beta\alpha}) + \varphi_i(z',s_{12}^{\beta'\alpha'})] + \varphi_i(z,1_2^\alpha) + \varphi_i(z',1_2^{\alpha'}) + \varphi_i(z,N_{i1}^\alpha) + \varphi_i(z',N_{i1}^{\alpha'}) \right\}. \end{aligned} \tag{17}$$

In this way every bond is counted half from one end, the segment with the lower ranking number, and half from the other end, the segment with the higher ranking number. End segments have only one bond connected to them and therefore only one-half the densities of the end segments add to the sum. The volume fraction of the end segments of molecule i in layer z with its bond in direction α, $\varphi_i(z,1_2^\alpha)$, and $\varphi_i(z,N_{i1}^\alpha)$, are calculated through

$$\begin{aligned} \varphi_i(z,1_2^\alpha) &= C_i\lambda^{\alpha\beta}G_i(z,1_2^\alpha) \\ &= C_i\lambda^{\alpha\beta}G_i(z,1^\alpha)G^{\alpha''}(z|z')\sum_{\beta\neq\alpha}\frac{1}{3}G_i(z',2_2^{\alpha\beta}), \end{aligned} \tag{18}$$

$$\varphi_i(z,N_{i1}^{\alpha}) = C_i \lambda^{\alpha\beta} G_i(z,N_{i1}^{\alpha}) = C_i \lambda^{\alpha\beta} G_i(z,N_i^{\alpha}) G^{\alpha''}(z|z') \times \sum_{\beta\neq\alpha} \frac{1}{3} G_i(z',[N_i-1]_1^{\beta\alpha}).$$

The propagator method for branched flexible chains is slightly more involved than for linear flexible ones.[17] The only difference is at the branch point. There, not two end segment weighting factors are connected to each other, but three or more, as defined by the chain architecture:

$$\varphi_i(z,s_{123\cdots}^{\alpha\beta\gamma\cdots}) = C_i \lambda^{\alpha\beta} \frac{\Pi_{\sigma'} G_i(z,s_{\sigma'}^{\alpha\beta\gamma\cdots})}{G_i(z,s)^{N_{\sigma si}-1}}. \tag{19}$$

The three dots $(\cdots)$ indicate the possibility that more than three bonds are present on the segment s. The bonds connected to segments s of molecule i are numbered from $\sigma' = 1,2,...,N_{\sigma si}$, where $N_{\sigma si}$ is the number of bonds on segment s of molecule i.

The end segment weighting factors in Eq. (19) are obtained again by Eq. (15). Only the probability for the specific local bond conformation $\lambda^{q_{\sigma i}}$, just near the node, can no longer be expressed in *gauche* and *trans* conformations. The end segment weighting factor for a segment s next to a branch point is calculated by an equation, which, in a sense, is a mix between Eqs. (15) and (19). In fact, one should realize that the unnormalized volume fraction of the branch point [cf. Eq. (19)] is needed (several chains are connected), but that one chain branch is not yet connected; and this branch is now to be propagated [cf. Eq. (15)]. In other words, the bond, σ, between the branch point s' and the segment s next to the branch point remains to be ''made.'' For this, the free segment weighting factor of the segment s is multiplied by the anisotropic weighting factor for bond σ and the sum of the probabilities of finding the branch point, s', with all bonds (σ', σ'', etc.) but one (i.e., the one, σ, that is to be made) connected, weighted by the probability of the local bond conformation of the newly ''made'' bond. Mathematically this is expressed as

$$G_i(z,s_2^{\alpha\beta}) = G(z,s) G^{\beta''}(z|z') \times \sum_{q_{\sigma i}^{\alpha''-\beta''-\cdots}} \lambda^{q_{\sigma i}^{\alpha''-\beta''-\cdots}} \frac{\Pi_{\sigma'\neq\sigma} G_i(z',s'^{\beta'\cdots}_{\sigma'})}{G_i(z',s')^{N_{\sigma s' i}-2}}. \tag{20}$$

The sum over $q_{\sigma i}^{\alpha''-\beta''-\cdots}$ is over all local bond conformations with bond σ in molecule i as the central bond that have orientation β'' for bond σ and orientation α'' for the other bond on segment s, away from the branch point (bond σ°, Fig. 3).

Branched molecules contain more that two chain ends. Each branch in the chain has an end unit, which, at some point in the scheme, is the starting point of the propagator scheme. These cases are obviously handled by Eq. (16).

The fraction of maximum bond density, $\varphi^{\alpha''}(z|z')$, has, compared to Eq. (17), extra terms for every segment that has an extra bond connected to it and also an extra sum over these extra bonds. For instance, for a system with molecules with some segments that possess three bonds, Eq. (17) becomes

$$\begin{aligned}\varphi^{\alpha''}(z|z') = \frac{1}{2}\sum_i \Bigg\{ & \sum_s [\varphi_i(z,s_1^{\alpha}) + \varphi_i(z',s_1^{\alpha'})] \\ & + \sum_{s'}\sum_{\beta''} [\varphi_i(z,s'^{\alpha\beta}_{12}) + \varphi_i(z',s'^{\beta'\alpha'}_{12}) + \varphi_i(z,s'^{\beta\alpha}_{12}) \\ & + \varphi_i(z',s'^{\beta'\alpha'}_{12})] + \sum_{s''}\sum_{\beta''}\sum_{\gamma''} [\varphi_i(z,s''^{\alpha\beta\gamma}_{123}) \\ & + \varphi_i(z,s''^{\beta\alpha\gamma}_{123}) + \varphi_i(z,s''^{\gamma\beta\alpha}_{123}) + \varphi_i(z',s''^{\alpha'\beta'\gamma'}_{123}) \\ & + \varphi_i(z',s''^{\beta'\alpha'\gamma'}_{123}) + \varphi_i(z',s''^{\gamma'\beta'\alpha'}_{123})] \Bigg\}. \end{aligned} \tag{21}$$

Here s denotes the end segments, with one bond, s' refers to the ordinary segments having two bonds, and s'' indicates the segments with three bonds connected (the branch points). For systems that have molecules that contain branch points with more than three bonds connected to it, Eq. (21) has to be replaced by an equation with even more terms.

We now turn our attention to the extensions of the propagator scheme for molecules that contain rigid fragments. Several problems arise as the bond lengths or the bond angles are not all necessarily uniform. In these cases segments will not automatically be situated at the center of a lattice layer. Since the segment potential field is, in essence, a step profile we choose to let the segment feel the potential field in the layer where its center resides. This approach was also followed by several authors in the literature,[12–14] when they determine the local potential for a chain conformation. The same applies to end segment weighting factors: the end segment is assumed to be in the layer closest to its actual position. The contribution of a segment to the volume fraction profile, on the other hand, is subdivided over the layers that it spans. We have distributed the segment volume fraction over two neighboring layers when the segment position was not exactly on a lattice site. To calculate similarly the end segment weighting factor for a given segment s, on a position not at the layer center, as a combination of the end segment weighting factor for the two neighboring layers, has its problems. If we ignore for a moment chain stiffness aspects and the anisotropic field, the end-segment weighting factor is the sum of the weighting factors of all conformations of the piece of chain ending with the segment s on a nonlattice site position. The weight of one conformation is the product of the Boltzmann factors of its constituent segments [Eq. (8)]. The Boltzmann factor is the exponential of the local segment potential field [Eq. (9)]. So the end segment weighting factor is a sum (over all conformations) of the product (over all segments) of exponentials of the segment potential fields. The end segment weighting factor of a segment not on a lattice layer should be the sum (over all conformations) of the product (over all segments) of expo-

nentials of the *averaged* segment potential fields. To do this, the whole recursive scheme should be run for every off-lattice position of a segment in a rigid structure for every conformation. This would destroy the efficiency of the propagator scheme completely. Therefore we have used, as a first approximation, the end segment weighting factor for the segment as if it were located at the center of the layer closest to the center of the segment (z_r).

Bond angles are not always parallel to the tetrahedral bonds in the lattice either. We chose a similar solution to this problem as for the segmental coordinates: for every conformation of the structure each bond that has an angle with the lattice plane larger than 45° is considered to be in the direction *h*, every bond, which angle is smaller than −45° is assumed to be in the direction *e* and all other bonds are equally divided between the directions *f* and *g* (isotropic approximation within the layer).

When incorporating rigid (ring) structures, not only the directions of the bonds connecting the segments that are part of the structure itself have to be defined, but also the directional information for the bonds of the substituent chain parts, linking these flexible chains to the ring, needs to be given. In this way we prevent direct back-folding of the flexible chain onto the rigid fragment. In a Markov approximation the number of conformations of a flexible chain part is strongly dependent on $N[\propto(Z-1)^N]$. For rigid structures the number of conformations that we include is only linear in the number of segments and therefore we proceed by calculating every conformation of the ring explicitly. What is done for the rigid fragments resembles the calculation of the statistical weight of all possible local conformations of a set of three consecutive bonds in the linear chain case, because any three consecutive segments in the ring determine all the other coordinates of the ring units.

The various rigid structures in a molecule are denoted with the letter $k=1,2,...$, which each include N_{ki} segments. The local conformations of structure *k* in molecule *i* are denoted as q_{ki}. To generate the full set of conformations of a rigid structure *k*, the following procedure is followed (for full details see the Appendix) for *each* segment s_k, a member of the structure *k*.

The given relative coordinates of the structure are translated in such a way that segment s_k is in the origin of an arbitrary continuous Euclid three-dimensional (3D) space with a Cartesian coordinate system with unit vectors of length *l*. Next, two independent orthogonal vectors that describe the orientation of the structure are connected to s_k. Once these two vectors are known, six well-defined orientations of the structure are generated by rotation around the origin (i.e., the position of segment s_k). The *z* coordinates in the continuous system of all segments in the structure, which need not be integers, are then projected into the lattice system such that segment s_k is exactly at the center of a given layer *z*.

Since the segments are not always positioned at the center of a lattice layer we use *r* as the noninteger *z* coordinate, normalized on the lattice spacing *l* of the center of such a segment. The layer that is closest to the center of the segment at position *r* is denoted as z_r.

To distribute the volume fraction of a segment over several layers the fraction of the segment volume of a given segment *s* in layer *z* is defined, depending on the conformation, q_{ki}, of the structure *k*, of which *s* is a member. This fraction is denoted as $f^{q_{ki}}(z,s^\alpha)$, where the superscript α selects only those conformations that have an outgoing bond on segment *s* in direction α (cf. Fig. 3). This fraction is calculated as if a segment had a cubic shape. So, if segment *s* in structure *k* in conformation q_{ki} has a position *r*, the fraction of the segment in the layer closest to its center, z_r, is $f^{q_{ki}}(z_r,s)=1-|r-z_r|$. The fraction of the volume of the segment in the next neighboring layer is then $|r-z_r|$. Since the segments have the size of the lattice spacing they cannot span more than one layer and, consequently, $f^{q_{ki}}(z,s^\alpha)$ has only nonzero values for the above-mentioned two neighboring layers.

The sum of $f^{q_{ki}}(z,s^\alpha)$ over all conformations q_{ki} and all directions α gives the number of structure conformations relevant for the volume fraction of a segment *s* that is a member of the structure *k* at layer *z*, $N_{q_{ki}}$. The symbols *z* and *s* are dropped because this number is independent of the layer number *z* and the segment number *s* of structure *k*:

$$N_{q_{ki}}=\sum_{\alpha}\sum_{q_{ki}} f^{q_{ki}}(z,s^\alpha)=6N_{ki}. \tag{22}$$

Below we will need a normalizing factor for the sum of these conformations, $\lambda^{\alpha k}$. This factor is, in essence, part of the local bond probability for the bond on segment *s*, $\lambda^{q_{\sigma i}}$. As a first approximation we take the energy for rotation around the bond σ_0, connecting a flexible chain to the structure *k*, constant for all local conformations (no *gauche–trans* energies for σ_0). With this ansatz the normalization factor is the inverse of the number of local conformations of structure *k* corrected for the *a priori* chance to find the outgoing bonds in direction α: $\lambda^{\alpha k}=Z/(N_{q_{ki}})$, where, as before, *Z* represents the number of different bond directions in the lattice.

Now, to calculate the volume fraction, $\varphi_i(z,s_{1k}^\alpha)$, of this segment *s* in structure *k*, we have to sum over all conformations of the structure and select those that have a fraction of segment *s* in layer *z* with the outgoing bond on segment *s* in direction α. The weight of each conformation is determined by the product of the end segment weighting factors, $G_i(z_r',s_1'^{\beta''})$, of the segments s' belonging to the structure, and the anisotropy weighting factors $G^{\sigma'}(z'|z'')$ for all the bonds, σ', in the structure, where z' and z'' are determined by the position and the direction of the bond in the specific conformation. As mentioned above, if the bond σ' makes an angle with the lattice plane that is larger than 45° $G^{\sigma'}(z'|z'')$ becomes equal to $G^{h''}(z'|z'')$, if the angle is between −45° and 45° it becomes $G^{f''}(z'|z'')$, but if the angle is smaller than −45°, $G^{e''}(z'|z'')$ is substituted. There is a special case if a bond σ' in orientation f'' or g'' starts in layer z', but ends in another layer, z''. This can easily occur due to a finite angle of the bond with the lattice plane. In this case the anisotropy weighting factor for that bond is averaged over the two layers. For example, for σ' in direction f'': $G^{\sigma'}(z'|z'')=\frac{1}{2}G^{f''}(z'|z')+\frac{1}{2}G^{f''}(z''|z'')$.

All told, the anticipated equation reads as

$$\varphi_i(z,s_{1k}^{\alpha})=C_i\sum_{q_{ki}}\left(\lambda^{\alpha k}f^{q_{ki}}(z,s^{\alpha})\prod_{s'\in k}G_i(z_r',s_1'^{\beta''})\times\prod_{\sigma'\in k}G^{\sigma'}(z'|z'')\right)_{q_{ki}}. \tag{23}$$

The subindex $1k$ in s_{1k}^{α} denotes that segment s has a chain end connected to the outgoing bond 1 in direction α and that structure k is connected to this segment as well. The subindex q_{ki} of the large parentheses infers that all positions and directions of bonds and the coordinates of the segments within the brackets are determined by the conformations q_{ki}. Obviously, if on a unit in a structure no flexible constituent is attached, it suffices to include the free segment weighting factor for this unit instead of the end segment weighting factor in Eq. (23).

The propagation step to compute the end segment distribution of a segment s member of a flexible chain part next to the rigid structure is analogous to that of the segment next to a branch point. It involves the calculation of the unnormalized volume fraction of the segment s' in the rigid structure k, onto which the flexible chain will be connected, with the outgoing bond in the direction that the propagator will follow. Let s'' denote the other segments in the structure to which the flexible chain is not connected; then the propagator step can be written as

$$G_i(z,s_2^{\alpha\beta})=G_i(z,s)G^{\beta}(z|z')\times\sum_{q_{ki}}\left(\lambda^{q_{\sigma i}}f_r^{q_{ki}}(z',s'^{\beta})G_i(z_r',s')\times\prod_{(s''\neq s')\in k}G_i(z_r'',s_1''^{\gamma'})\prod_{\sigma'\in k}G^{\sigma'}(z''|z''')\right)_{q_{ki}}. \tag{24}$$

In Eq. (24) z'' denotes the positions of the segments s'' depending on the conformation q_{ki} and σ' denotes the bonds in the fragment k. The factor $f_r^{q_{ki}}(z',s'^{\beta})$ equals unity if $z'=z_r$ for segments s' with outgoing bond β in structure k in conformations q_{ki} and zero otherwise.

In previous sections we have shown how to calculate $\varphi^{\alpha''}(z|z')$ for linear and branched semiflexible chains [cf. Eqs. (17) and (21)]. The same quantity has to be computed in the case that rigid structures are part of the molecules in the system. In Eq. (21) three terms are present, accounting for segments with one, two and three bonds, respectively. Segments in a rigid structure often have two or three bonds connected to it. Consequently, they contribute to the corresponding terms in Eq. (21). If there are segments present in the rigid fragment that have more than three bonds, Eq. (21) has to be expanded with extra terms analogous to the case of branch points where four chain parts come together.

D. Computational aspects

Mirrorlike lattice boundary conditions ensure through Gauß' law the electroneutrality of the system[19,30] and provide a way to eliminate the translational degrees of freedom for the bilayers (the midplane of a bilayer is positioned at the boundary of the system by means of a suitable initial guess in the numerical solver). Rigid structures can have relative positions that span more than one lattice layer and hence can sample coordinates $z'<0$ and $z'>M+1$, while having at least one of their units between the layers $1\leqslant z''\leqslant M$. The potential felt at these coordinates z' follow from the reflecting boundary conditions. These are realized by putting the field $u(1-z)=u(z)$ and $u(M+z)=u(M+1-z)$ for all z. For linear and branched chains only potentials at layers $z=0$ and $z=M+1$ are required for the calculations.

From the above it follows that the density distributions can be computed from the segment potentials and the bond weighting factors. Both the segment potentials and the bond weighting factors can be derived from the density distribution. The fixed point of the equations is known as the self-consistent-field solution and is found numerically. Only a solution that obeys the incompressibility constraint [$\Sigma_A\varphi_A(z)=1$ for every z] is accepted. Typically the precision of the resulting potentials is better than seven significant digits. For the lipid (and the additive) a canonical partition function is evaluated, which means that the normalizing constant C_i is calculated through Eq. (13). For water and ions the environment is considered open, hence the approach is grand canonical and C_i follows from Eq. (12). Once the equilibrium profiles are known we can evaluate the partition function from which all mechanical and thermodynamic quantities follow.

Membranes calculated in this way have, in general, a finite surface tension. The equilibrium conditions of a free-standing membrane can be deduced from the thermodynamics of small systems, as pioneered by Hill[31] and applied by Hall and Pethica.[32] From this theory it follows that the membrane surface tension must be balanced by entropic contributions originating from translational and undulational degrees of freedom. Typically membranes are very large and thus their translational entropy is relatively small. Furthermore, biological membranes are rather stiff, so that the out-of-plane bending can, to a good approximation, be neglected.[33–35] It should therefore be concluded that the surface tension of lipid bilayers must vanish. In the calculation scheme this is realized by changing the amount of lipid per unit surface area (θ_{lipid}) iteratively until $\gamma=0$. The surface tension or excess free energy per unit area of the membrane are a function of the density and the potential profiles as well as the anisotropic weighting factors. The equation has been derived before[19] and is without modifications applicable for the present system.

E. The partition coefficient

The partition coefficient K_i is defined as the ratio between the amount of additive i per amount of lipid in the membrane and the same for the additive in the water phase:

$$K_i(\mathrm{id}) = \frac{(\varphi_i/\varphi_{\mathrm{lipid}})_{\mathrm{membrane}}}{(\varphi_i/\varphi_{\mathrm{water}})_{\mathrm{water}}}, \tag{25}$$

where the index on φ indicates the species and the index in the parentheses the phase involved. The extension ''id'' refers to the ideal definition of K_i to be distinguished from the pragmatic definition, to be explained below. Since there are several ways to express the concentration of a substance, the partition coefficient can be defined in as many ways. Our measurements are set up in such a way that the partition coefficients are calculated as the quotient of the weight percent of additive in the bulk and that in the membrane phase. We assume that the specific densities of water and lipid are equal, which allows us to calculate the partition coefficient on the basis of volume fractions.

Experimentally, the partition coefficient can be measured from the change in concentration of the additive in the water phase upon addition of the lipids. Thus, essentially the partition coefficient of an additive with respect to the partition coefficient of water is calculated. Note that in this way $K_i(\mathrm{exp})$ can assume a negative value if water partitions more favorably into the membrane than does the additive. In this case one would experimentally measure a concentration increase of the additive upon addition of the lipids. However, for most investigated additives $K_i(\mathrm{exp})$ remains positive, but, for example, $K_i(\mathrm{exp})$ is typically negative for small ionic species that do not complex with the head groups of the lipids.

A problem in calculating the partition coefficient from our numerical density profiles is to define the extent of the membrane phase. The membrane boundary is hard to define, as there is no sharp interface between bulk water and the membrane. We define the volume of the membrane as the excess volume of lipids in the system, neglecting thereby the swelling of the membrane by water or by other species. This approach is also used in the experimental setup. The amount of an additive in the membrane is defined as the excess amount of additives in the system plus the bulk concentration times the volume of the membrane phase. Defining the excess amount with respect to the bulk solution per surface area of the membrane as θ^{exc} we arrive at the following expression for $K_i(\mathrm{th})$:

$$K_i(\mathrm{th}) = \frac{(\theta_i^{\mathrm{exc}} + \theta_{\mathrm{lipid}}^{\mathrm{exc}} \cdot \varphi_i^b)\varphi_{\mathrm{water}}^b}{\theta_{\mathrm{lipid}}^{\mathrm{exc}} \cdot \varphi_i^b}. \tag{26}$$

In the following we will drop the extension ''th,'' as it will be clear that we have used Eq. (26) to compute this value.

F. Parameters

The theory discussed above is implemented in a computer program called GOLIATH. The membrane, for which the results in this paper were generated, consists of DMPC molecules, as shown in Fig. 4. This membrane is embedded in a solution of monomeric isotropic molecules mimicking water, wherein monovalent salt ions, referred to as Na^+ and Cl^-, are present. The volume fraction of salt in all calculations was fixed to $\varphi_s = 0.002$, which is comparable to a concentration of about 50 mM.

TABLE II. The parameters of the various segment types considered in this study.

		H_2O	C	O	S	PO	N	Na	Cl
ϵ_r		80	2	80	80	80	80	80	80
ν		0.0	0.0	0.0	−1.0	−0.2	+1.0	+1.0	−1.0
χ	H_2O	0.0	1.6	0.0	−1.0	−1.0	−1.0	−1.0	−1.0
	C	1.6	0.0	1.6	2.6	2.6	2.6	2.6	2.6
	O	0.0	1.6	0.0	0.0	0.0	0.0	0.0	0.0
	S	−1.0	2.6	0.0	0.0	0.0	0.0	0.0	0.0
	PO	−1.0	2.6	0.0	0.0	0.0	0.0	0.0	0.0
	N	−1.0	2.6	0.0	0.0	0.0	0.0	0.0	0.0
	Na	−1.0	2.6	0.0	0.0	0.0	0.0	0.0	0.0
	Cl	−1.0	2.6	0.0	0.0	0.0	0.0	0.0	0.0

A set of linear alcohols (from butanol up to octanol), several branched alcohols with seven carbon atoms, para alkyl-substituted phenols, and a few linear alkyldiols were used to compare the theoretical predictions of the model with experimental data. For all the other additives only theoretical predictions are available. We analyze the behavior of a set of isomers containing two charged groups, one segment with a positive charge, denoted as N^+, and one with a negative charge, denoted as S^-, positioned on a alkyl chain of 16 C units connected to a benzenelike ring with bond lengths equal to the lattice spacing l (see Fig. 4, additive 1 and 2 for two examples). In addition, calculations are performed for tetrahydroxy naftalenes with the four hydroxyl groups substituted in various ways around the ring system (see also Fig. 4 for an example). Note that the letter *S* used as a generic name for a negatively charged group should not be confused by the element sulphur, it merely is used as a unit with similar properties as the *N* but with opposite charge.

The system size was chosen large enough to prevent bilayer interaction (usually $M = 40$ layers). The lattice spacing, l, was set to 0.3 nm. The energy difference between a *gauche* and a *trans* state (in a linear chain part) and between the *gauche–gauche* and the *trans–gauche* state (at a branch point) was set to 1 kT, irrespective of the segment types involved. Further segment properties were chosen, as given in Table II. The relative dielectric constants of all components, except for the hydrocarbon (C), were taken as $\epsilon_r = 80$, the value found for bulk water. For hydrocarbon the value $\epsilon_r = 2$ was chosen, corresponding to the value found for bulk hydrocarbon fluids.

Regarding Table II, the contact energy between hydrocarbon and water, reflected in $\chi_{\mathrm{C,H_2O}}$ is the most critical parameter for membrane formation as it is the driving force for self-assembly. The value was chosen to be $\chi_{\mathrm{C,H_2O}} = 1.6$, similar to that validated by earlier studies[17,19,20,23] and in accordance with other estimates found in the literature.[36] This value was found by comparing theoretical predictions of the critical micellar concentration (CMC) as a function of the surfactant tail length with experimental data.[18] We note that we did not introduce energetic differences between a C in a flexible chain and C in a ring. The χ value for uncharged

polar segments (O) with respect to hydrocarbon (C) was set equal to the water–hydrocarbon value. Charged components (N, Na, Cl, P, S and the O from the phosphate group) are assigned a favorable χ of -1 with water to mimic their tendency to be solvated by water and an unfavorable one with the hydrocarbons of $+2.6$ for the lack of solvation in hydrocarbon. The other interactions are not critical and their χ values are kept zero for the sake of simplicity.

The phosphate group is modeled as being composed of five units. Since this group has a low intrinsic pK_a value of <2.25,[37,38] it has a net negative charge of -1 at neutral pH. This charge is assumed to be equally distributed over all five segments. Thus, effectively we put a charge of -0.2 on each of these units.

III. RESULTS

In the following a selection of results for free-standing liquid crystalline DMPC membranes will be discussed. This information is of importance to interpret the behavior of additives in it. In the remainder of this section we discuss this membrane perturbed by three groups of relatively simple additives.

A. Free-standing liquid crystalline DMPC bilayers

The first lipid membranes that were investigated several years ago with a SCF analysis were rather primitive. The lipids were modeled as simple molecules with two long hydrophobic tails of 16 hydrocarbon segments and a hydrophilic head group of five structureless units. Isotropic, structureless monomers were used to model the water molecules.[17–19] The trends found for the tail region of the membrane are very similar to the results found in the modern calculations. The gel to liquid phase transition could be reproduced and details in the segment positions in the tail region have been predicted. The width of the distribution of tail segments increases the further the tail units are positioned away from the head group–tail boundary in the molecule. In line with this, it was found that the sn_1 tail is positioned a fraction of a nm deeper into the membrane core than the sn_2 tail (see Fig. 4). With respect to the head groups it was found that the maximum in their volume fraction profile was never higher than 0.3. This implied that even in the so-called head group region the most predominant segment–segment contact is the hydrocarbon–water one. We note that in all these calculations the membrane surface tension was kept to zero at all times, as should be the case for free-standing bilayers.

In Fig. 5 we present the SCF prediction of the structure of model membranes composed of DMPC molecules. The molecular structure of DMPC is more detailed, and the head group is bulkier as compared to the lipids considered earlier. Again, the total head group volume fraction profile never exceeds the value of 0.3 for equilibrium membranes and again the most frequent contacts in the head group region are the hydrocarbon–water ones. The head groups do not form a neatly packed layer shielding the hydrocarbon tails from the aqueous environment. Upon closer inspection, the head group is found lying predominantly flat on the membrane surface.[20,23] This result is in good correspondence with

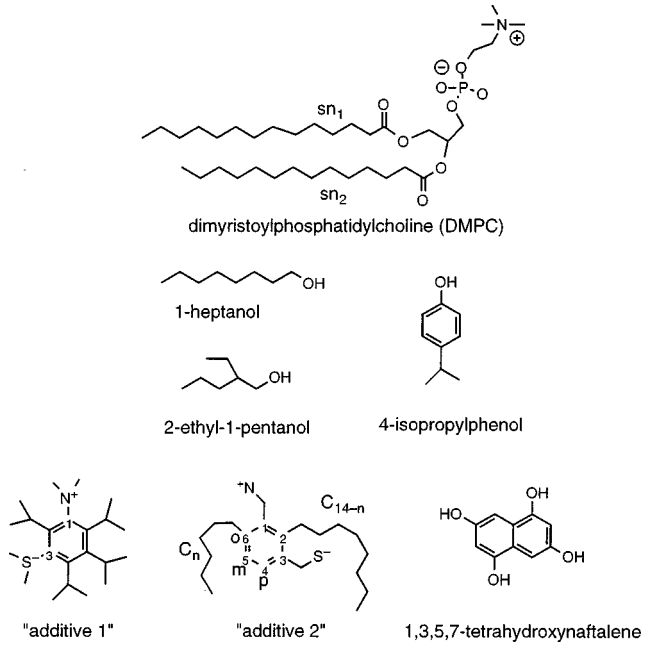

FIG. 4. Some of the molecules considered in this study. DMPC makes up the lipid matrix of the membranes and the other molecules are additives. Note that the letter *S* is used for a unit that mimics the properties of an *N* but has the opposite charge; it should not be confused with the element sulphur.

experiments[24] and other theories.[4,39,40] Generally, at moderate salt concentrations, the outer part of the head group, the choline moiety, has a wider distribution than the phosphate group, which is closer to the head group–tail interface in the molecule. Moreover, it is found that, at high salt concentrations, the choline assumes a two-state distribution around the phosphate (not shown). This is interpreted in such a way that the head group has two preferred conformations: one with the choline closer to the hydrocarbon core of the membrane than the phosphate, and one with the choline closer to the water phase. This situation was also encountered in experiments.[24]

Due to the out of plane tilting of the head groups an electrostatic potential profile develops (see Fig. 5) with a negative value in the head group region on the position of the phosphate group and a positive value in the center and on the outskirts of the membrane. Due to this profile, anions and cations distribute differently over the membrane phase. Both ions are expelled from the hydrophobic core due to the bad solvent quality of the hydrocarbon tails of ions, but anions are less expelled than cations. This can be part of the explanation for the difference in permeability between anions and cations through DMPC membranes.

B. Partition coefficients of alcohols

To compare our theory with experimental results the partition coefficients for linear and branched alcohols and those for phenols were computed according to Eq. (26) and measured according to the scheme explained in the experimental section; see Eq. (27). The results are shown in Fig. 6. There are two main features that are striking. The first is that nearly all points are on the diagonal, indicating that the theory pre-

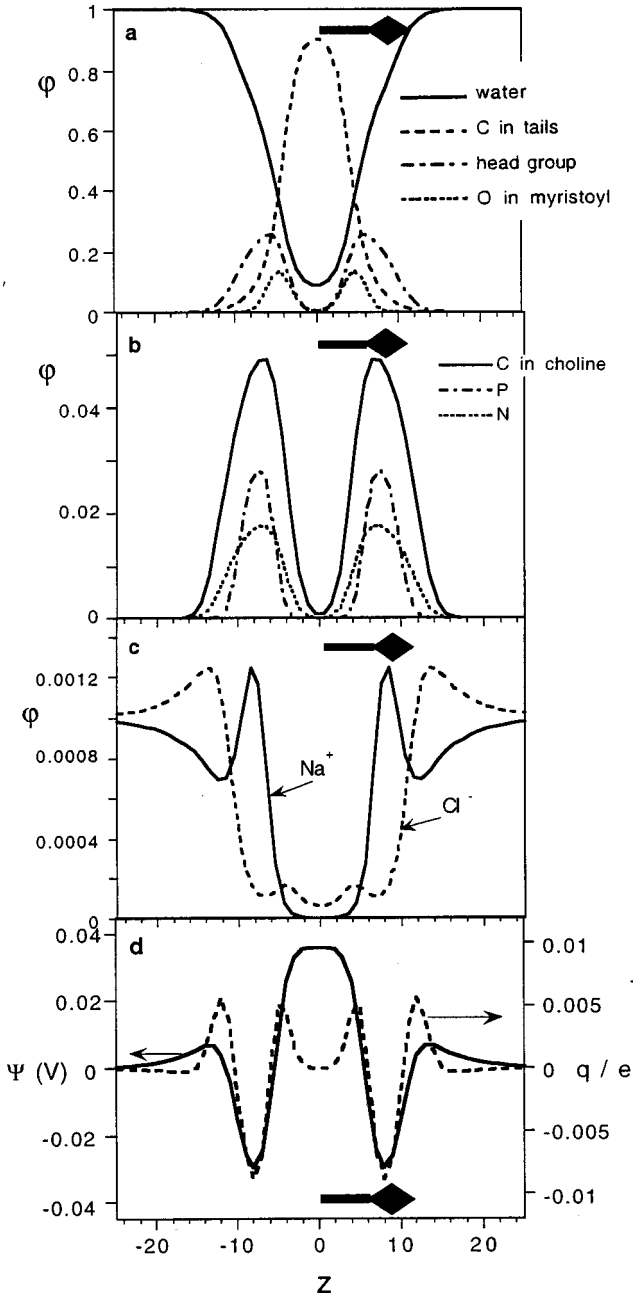

FIG. 5. The volume fraction, φ, charge distribution, q, and electrostatic potential, Ψ, profiles through a cross section of an undoped free-standing liquid crystalline DMPC membrane. The director shown in every diagram is perpendicular to the membrane surface, indicating the hydrophobic core with its tail and the head group area with its head. The volume fraction of salt solution in the bulk is 0.002, the relative dielectric constants, valences, and χ parameters are as in Table II. The center of the membrane is at $z=0$.

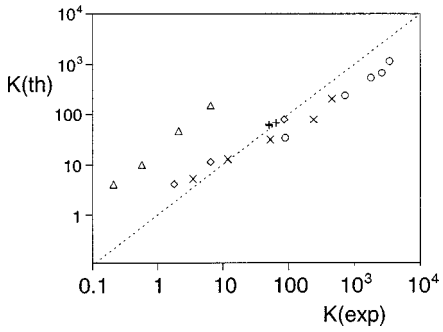

FIG. 6. The comparison between the partition coefficient of our theory and the experiments, for several groups of alcohols. Crosses: linear -1-alkanols from low K values to high: 1-butanol, 1-pentanol, 1-hexanol, 1-heptanol, and 1-octanol. Plusses: branched alkanols with seven carbon atoms: 4-heptanol, 2,4-dimethyl-3-pentanol and 2-ethyl-1-pentanol; linear alkane diols are divided into two groups 1,2-alkanols shown as diamonds: 1,2-pentanediol, 1,2-hexanediol and 1,2-octanediol and 1,n-alcanediols shown as triangles: 1,5-pentanediol, 1,6-hexanediol, 1,7-heptanediol, and 1,8-octanediol. The circles are several para-substituted phenols in order of the increasing K value: phenol, 4-ethyl; 4-isopropyl, 4-propyl and 4-tert.butyl phenol. The additive concentration in the membrane was about 1.5 vol %. Salt concentration and other parameters were the same as in Fig. 5. The experimental data are unpublished results kindly provided to us by Van Lent at Bayer AG, Leverkusen.

dicts the correct value, and the second feature is the deviation of the 1,n-alkanediols from this diagonal (which indicates a problem).

The first observation is surprising since *no* parameter fit of any kind was performed to match the experimental partition coefficients with the theoretical ones. Moreover, our parameter set is still quite crude. For instance, there is a known difference between CH_3 and CH_2 groups that is not accounted for in our approach. It can be concluded that apparently these differences are of minor importance in predicting the partition coefficients.

The systematic underestimation of the theoretical values for the 1,n-alkanediols as compared with the experimental ones is probably due to the fact that in the theory the molecules in homogeneous water solutions cannot develop any specific inter- or intramolecular interactions. This means that, for example, 1,2-pentanediol has the same activity as 1,5-pentanediol if these molecules have the same bulk concentration. In our model the chemical potentials of two isomers with the same bulk concentration within the same overall bulk composition are identical. This might not be the case in practice. There are probably specific interactions that causes one molecule to like the water phase better than the other one. An indication that this is playing a role is the difference in solubility between the two: 1,2-pentanediol has a solubility of 1.3 grams per liter while the solubility for 1,5-pentanediol is 0.8 grams per liter. Therefore we conjecture that the predictive power of our model will increase when our theoretical predictions are combined with experimental data on, e.g., octanol/water (O/W) partitioning. With information on O/W partitioning one can correct for activity effects of additives in the homogeneous water phase.

It appears that, for these relatively small molecules, the molecular architecture is not of main importance for the partitioning into the membranes as long as there are no specific intramolecular interactions in the water phase. The addition of a hydrophobic (hydrocarbon) segment or a hydrophilic (hydroxyl) segment has a considerably larger effect than branching or the incorporation of a para-substituted benzene ring. In a homologue series of molecules (e.g., n-alcohols), the addition of one C segment increases the partition coefficient with a factor of approximately 3. Clearly changing the architecture while keeping the overall composition constant

has only secondary effects on the membrane–water partition coefficient.

Comparing in Fig. 6 the theory with the experiments for the partition coefficient in some more detail, we notice that the theory underestimates K for the linear molecules more than for the branched ones. For instance, the plus signs in Fig. 6, representing branched alcohols with seven carbon atoms, are located on the diagonal, i.e., here the theory predicts the experimental K correctly, while the fourth cross (1-heptanol) is located below the diagonal, indicating an under estimation of K by the theory. Branched molecules have more CH_3 groups than linear ones. Apparently the experimental results suggest that CH_3 groups reduce the partition coefficient. This can be because their packing efficiency in the ordered tail region is less than optimal due to their larger volume compared to CH_2's. Another possible explanation for this effect is that $\chi_{CH_3-water} < \chi_{CH_2-water}$, i.e., that the CH_3 interaction with water is more favorable than the CH_2–water one. Most frequently, however, it is assumed that CH_3 groups are more hydrophobic. Neither the size of a CH_3 group nor the difference in solubility of CH_3 and CH_2 in water are accounted for in our theory. Therefore we do not see dramatic effects in our calculations for K on chain branching.

From Fig. 6 it can be observed that the benzene ring of phenols increases the partition coefficient, in contradistinction to branching. In the first instance we would have expected that the effects of a ring on K would be the same as the introduction of branching, since it also introduces bonds that cannot line up with the main director of the lipid tails. On the other hand, a ring introduces one extra bond that receives an extra weighting through the bond weighting factors $G^{\alpha''}(z|z')$. This extra bond most likely causes the relatively high affinity of rings for the membrane phase. Upon closer inspection we observe that both in the experiments and in our theory 4-isopropyl phenol partitioned to a greater extent in the membrane than the *n*-propylphenol. The opposite was observed by Davis *et al.*, who measured the partitioning into gel state membranes.[41]

The volume fraction profiles of the additives of Fig. 6 do not contain many surprises. The carbon atoms pull several of the OH group of the alcohols into the center of the membrane. However, the density distribution of the OH still has a peak at the head group–tail boundary, which is more pronounced for molecules with longer hydrophobic tail lengths. Here we do not show density profiles for these additives; instead we refer to previously published results on dodecanol, which are typical.[42]

C. Partition coefficients, orientations, and positions of zwitterionic isomers

Let us next discuss the most symmetric isomers of the $C_{22}N^+S^-$ molecules. In Fig. 7 the partition coefficient is shown, as well as the average orientation of the molecules in the membrane. The orientation of the membrane is represented by the director, which was introduced in Fig. 5. All isomers have the positive charge on the rim of the hydrophobic core of the membrane close to the phosphate groups of the DMPC. Here the electrostatic potential is negative and the environment is relatively polar. When the two charges are spatially separated within the molecule, and thus when the local environment *in the molecule* is less polar, the average position of the positive charge within the membrane is located relatively close to the center of the membrane. The negative charge has less preference for a certain position in the membrane and is dragged into the membrane core if it is on the meta or para position on the ring with respect to the positive charge. This is not too surprising since the negative unit meets two forces: the membrane interior has a considerable positive electrostatic potential that attracts the negative charge whereas the hydrophobic nature of the core drives the negative charge to the water phase.

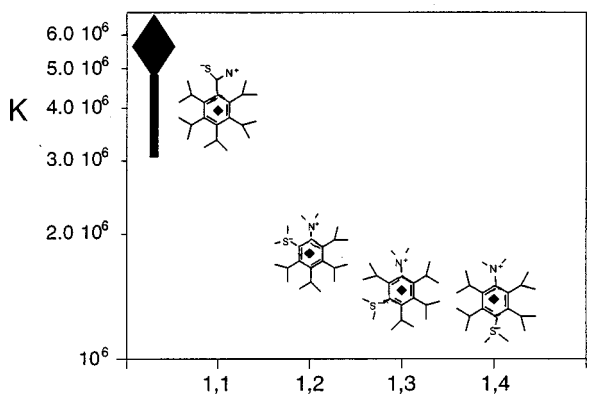

FIG. 7. The partition coefficient of four, nearly symmetric, isomers of the class $C_{22}N^+S^-$ molecules, indicated by the diamond inside the structure, are presented. On the *x* axis the positions of the substituents in the ring are indicated. The director indicates the size and direction of the membrane (cf. Fig. 5). The molecules as depicted represent schematically the average orientation of the additive in the membrane (see the director) with the positive charge close to the phosphates in the head group region (in the 1-position in the ring). The concentration of the additive in the membrane phase was about 0.1 vol %. Salt concentration and other parameters were as in Fig. 5.

With the relative positions of the positive and the negative charges in the molecule we can explain the differences in the partition coefficient between the four isomers. Note that this difference is as much as a factor 5, which is nearly equivalent to the effect that would be created by the addition of two carbon units (cf. Fig. 6). The fact that this difference is much larger than the differences in the partition coefficient due to structural changes in the group of alcohols discussed above can have several causes. The first one is that the isomers of Fig. 7 are larger structural units than most flexible molecules shown in Fig. 6. Second, all molecules in Fig. 7 are zwitterions. These molecules feel the electrostatic potential profile, which is strongly varying throughout the bilayer. The third reason is that in a rigid structure the variations in molecular architecture cannot easily be compensated. In flexible molecules rearrangements are possible and several compensation mechanisms can be envisaged. In rigid structures this is not possible and, especially in combination with the first point, substantial consequences of chain architecture for K should be expected. The deeper the negative charge is pulled to the hydrophobic core the lower is the partition coefficient.

To learn a bit more on the influence of the position of the

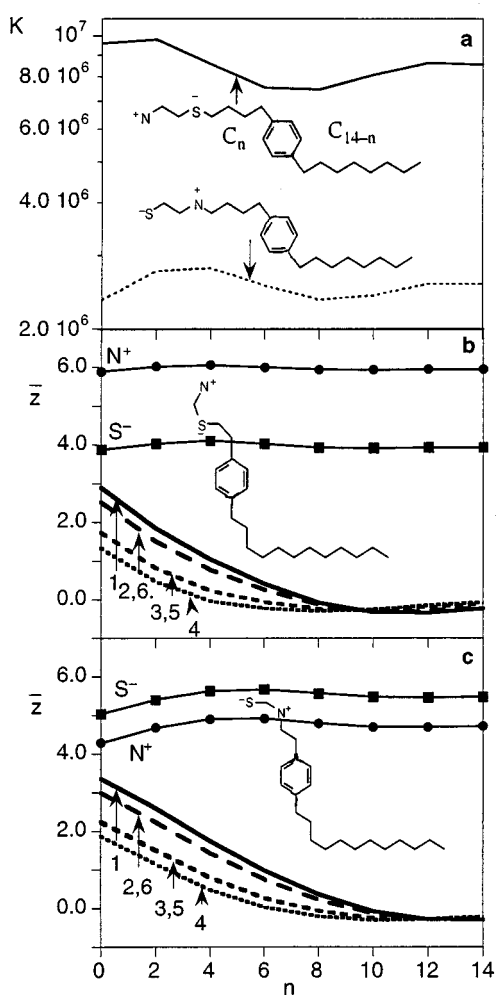

FIG. 8. Diagram (a) shows the partition coefficient of two types of molecules (as indicated) that differ in the position of the two charges as a function of the position of the ring in the chain. Diagrams (b) and (c) give the average positions of the charged and the ring segments of a set of isomers as depicted. The position of the ring is moved from close to the charges ($n=0$) to the end of the hydrocarbon chain ($n=14$). The amount of additive, the salt concentration, and all other parameters are the same as in Fig. 7.

positive and the negative charge in the molecule of this type of additive, we investigated the partitioning of the following subsets of the same type of isomers, as considered in Fig. 7. The two charges are now on the one end of the hydrocarbon chain separated by two C segments. The ring is positioned in the hydrocarbon chain (para substituted) and its position is moved from close to the charges to the other end of the chain. Two different series are calculated: one with the positive charge and one with the negative charge at the end of the chain. In Fig. 8 the results are summarized. In this figure we also give the molecular structure of these isomers.

The difference in partition coefficient upon switching positions of the two charges within the molecule is striking. The cause of this difference can be found by comparing Figs. 5 and 8. In Figs. 8(b) and 8(c) the average position $\bar{z}$ of the segments is plotted. These average positions are volume fraction-weighted average layers for the segment of type A involved and are calculated according to

$$\bar{z}_A=\frac{\sum_{z=-H}^{H} z\varphi_A'(z)}{\sum_{z=-H}^{H}\varphi_A'(z)}, \tag{27}$$

where H is the distance in layers between the two minima in the electrostatic potential profile due to the phosphates on both sides of the bilayer. H is typically about 20 layers and is a good measure for the (swollen) membrane thickness. By restricting the averaging in Eq. (27) from $-H$ to H we ensure that the whole membrane is taken into account and prevent that the bulk values do influence the average position too much. The volume fractions occurring in Eq. (27) are calculated from those conformations of the additive that had the positive segment restricted to one side (positive z values) of the membrane. The prime on φ therefore indicates that only a subset of all conformations is considered. If this restriction was not made, the average position would have been zero for all segments, since both sides of the symmetrical membrane contribute equally (see Ref. 19 for details).

From the average positions shown for various units in the additive (cf. Fig. 8), it can be deduced that the partition coefficient is largely influenced by the position of the positive segment. This is at the same time the segment that has the largest gradient in the segment potential field at its average position in the membrane. The segment potential field can easily be deduced from Fig. 5(c), where the ions, being monomeric molecules, follow the segment potential essentially according to a Boltzmann factor. The positive ion, Na^+, has the largest gradient between layers 4 and 8. Consequently, the statistical weight of conformations of molecules with positively charged units in this region, is very sensitive to the actual position of these units. Hence, the partition coefficient of these molecules is strongly dependent on the average position of the positively charged segment.

We note that this reasoning can only apply when the amount of additive in the membrane is so small that it does not influence the overall segment potential profiles. Upon an increase of the additive concentration in the bilayers the charge profile and other segment profiles can change considerably and potentially influence the partition behavior. These changes have then to be taken into account (see, e.g., Ref. 42).

The consequence of changing the average positions of the ring segments in the membrane are shown Figs. 8(b) and 8(c). A few noteworthy features can be observed. First of all, we recall that the ring is symmetrical with respect to the axis 1–4. This symmetry is reflected in the fact that segments 2 and 6 and segments 3 and 5 have exactly the same average positions. We mention this as evidence for the correct implementation of the propagation method for these structures. Second, at small n, i.e., a long tail at the 4 position of the ring, the normal of the plane of the ring is parallel to the membrane surface. The difference in average positions (i.e., in the direction perpendicular to the membrane surface) of segments 2 and 3 is close to 1 layer, which is the length of the bond between them. Third, the ring is pulled out more toward the water phase and the moreso with its normal parallel to the membrane surface, when the positively charged unit is closer to it, i.e., not on the end of the chain [Fig. 8(c)] but rather around $n\approx 4$. Again, two opposing forces are op-

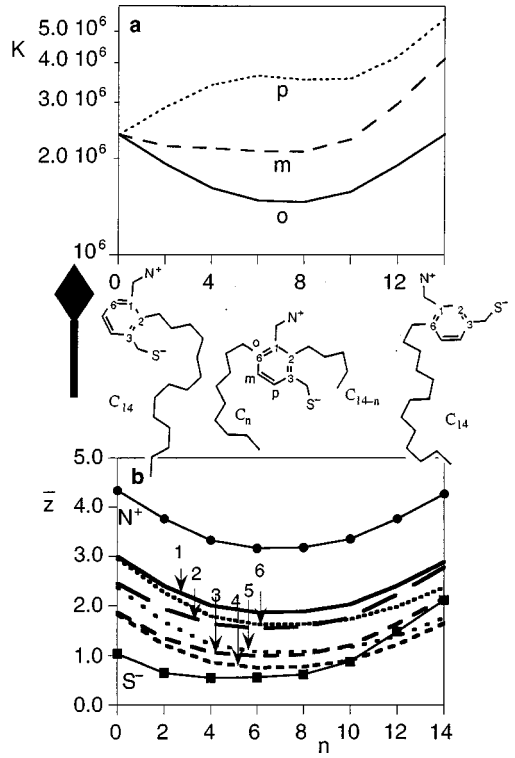

FIG. 9. Diagram (a) shows the partition coefficient, K, for the ortho- (o) meta- (m), and para- (p) substituted alkyl chain (see the text for details) as a function of the position of the ring in the alkyl chain. Diagram (b) shows the average position, $\overline{z}$, of the charged segments (N^+ and S^-) and the segments in the ring (1–6) of the ortho-substituted ring as a function of the position of the ring in the alkyl chain. The parameters are as in Fig. 7. The arrow indicates the director of the membrane (cf. Fig. 5).

erative in determining the position of the ring: the positive charge is pulled electrostatically to the phosphate group, whereas the apolar segments of the hydrocarbon tail prefer the membrane core and pull the ring to the center. These forces cause the ring to orient itself perpendicular in the membrane. Fourth, when the ring is at the end of the hydrocarbon chain the average positions of the units in the ring become all zero. This does not necessarily mean that the ring is lying flat in the membrane center. There are also conformations possible that pass the center and then return. In fact, this can be inferred from the $\overline{z}$ curve for ring-segment number 1 in Fig. 8(b). The position of this unit drops below the ones for the other ring segments for $n>9$. This can indicate two things: either the ring is for these molecules almost parallel to the membrane with a slight tilt, or several different conformations perpendicular to the membrane surface, and their mirror images exist so that the averaged positions are zero. This last possibility is probably true.

The third subset of the same type of isomers as in Figs. 7 and 8 that was investigated was designed as follows (see Fig. 9). The positive and the negative unit are attached to the ring with one carbon segment as a spacer, on meta positions with respect to each other. This moiety was then moved along a chain of 14 carbon segments. One end of the chain ($14-n$ segments long, with n between 0 and 14) is connected to the ring between the positive and the negative charge. The other end of the chain (n segments long) is connected to the ortho, meta, or para position with respect to the positive charge. In Fig. 9, three pictorial examples of the ortho-substituted chain are visualized. Their conformation represents (or at least mimics as well as possible) the theoretical prediction of the average conformation they assume in the membrane; cf. Fig. 9(b). Note that the fat arrow is again the director of the membrane indicating with its tail the hydrophobic core and with its head the head–group region of the membrane.

At $n=0$ the structures of all three (o, m, and p) isomers are identical, since in this case the o, m, or p chain is absent (see the left molecule in Fig. 9). For this molecule the orientation of the benzene ring is with the 1–6 bond almost parallel to the membrane surface. In this orientation the negative segment is forced toward the middle of the hydrophobic core of the membrane. The normal to the plane of the ring is almost parallel to the membrane surface. This can be concluded from the difference in average position between segments 1 and 3 in the ring, which is almost 1.3 layers, while their distance within the ring is about $1.7l$ (l is both the lattice spacing and the bond length in the ring). Upon increasing n, the number of carbon segments attached to the ortho position, the ring rotates around its normal and simultaneously the positive segment is drawn closer toward the membrane core. The occurrence of rotation can be inferred from the average positions of the ring segments: segments numbered 6 and 2 change z-positional order, just like segments numbered 5 and 3 do.

The rotation of the ring can be explained through the tendency of hydrophobic parts of a molecule to accumulate close to the membrane center. For small n, a hydrophobic tail is attached to the ring between the positive and negative charged units. As this ring tends not to lay flat on the membrane surface, it will pull at least one of the charges into the bilayer core. At $n>10$ the ring segment number 2 has only a few carbon segments attached to it. Now both charges are located near the membrane surface. We mention that when the ring is about halfway in the chain, the average position of the positive charge is located closest toward the bilayer center. Clearly the shape of the logarithm of the partition coefficient follows closely the average position of the positive segment. It first decreases upon increasing n and then for $n>10$ it increases again to almost the same value as for $n=0$.

The change in the partition coefficient of the meta- and the para-substituted isomers upon changing n can be explained along similar lines. The difference with respect to the ortho case is that the chain with n segments is located farther from the positive segment. Consequently, the hydrophobic segments are now moved from a chain close to the positive segment to a chain farther away from it, and therefore the surroundings of the positive charge within the molecule become more polar upon increasing n and its average position moves farther away from the membrane core. This increases K for those molecules at large n.

D. Partition coefficients, orientations, and positions of tetrahydroxy naftalenes

All ring structures discussed up until now showed the tendency to orient themselves with the ring–normal parallel to the membrane surface. To find out if it is possible to have rings oriented with the ring–normal perpendicular to the membrane surface, we have investigated the partitioning and orientation of some tetrahydroxy naftalenes. The orientation of the molecules is described by the angle between two vectors in the molecule with the plane of the membrane. One vector is directed along the short axis of the molecule: from unit 4 to unit 1 and the other is parallel to the long axis of the molecule: from unit 7 to unit 2. The angle $[\angle(c_1-c_4)]$ is defined as the angle of the vector between the average positions of the units 4 and 1 and the plane of the membrane, and it is calculated through

$$\cos\angle(C_1-C_4)=\frac{\overline{z}_{C_1}-\overline{z}_{C_4}}{d(C_1-C_4)}. \tag{28}$$

Here, C_1 and C_4 are the segments on position 1 and 4 in the structure, respectively, and $d(C_1-C_4)$ is the distance between the positions in the ring normalized on the lattice spacing l. The distance between, for instance, units 1 and 4 in a naphthalene structure is $2l$ (we have chosen the bond lengths to be equal to the lattice spacing). The calculation of the average positions was performed by selecting only those conformations that had the hydroxyl group on the 1 or the 2 position on the ring to one side of the membrane.

We present three members of the tetrahydroxy naftalenes that differ with respect to the positions of the OH groups over the rings. The first molecule that has been chosen has the OH's positioned two by two as far apart as possible: 2,3,6,7-tetrahydroxy naphthalene. In this case the molecule is, surprisingly, oriented spanning the membrane. Although the molecular dimensions are not really large enough to bring the hydroxyl groups in the head group area on both sides of the membrane, they are positioned close enough to the hydrocarbon–water interface so that they can make contact with the O segments of the myristoyl (of the DMPC) on both sides.

In the second molecule we consider the hydroxyls to be grouped to one side of the structure: 2,3,4,5-tetrahydroxy naphthalene. As compared with the previous example, the molecule rotated around the ring normal. The average position (cf. the pictorial of Fig. 10) of the hydroxyl groups is, on average, closer to the center of the head group region and, hence, the whole molecule moved more toward the water phase. The combined effect is that the partition coefficient is somewhat higher for this isomer as compared with 2,3,6,7-tetrahydroxy naphthalene.

For the third and last example considered, we have distributed the hydroxyl groups evenly over the molecule: 1,3,5,7-tetrahydroxy naphthalene (see Fig. 10). Now, the average orientation of the molecule is changed dramatically with respect to the previous two examples. The molecule now assumes an orientation with the plane of the rings almost parallel to the plane of the membrane. On average, it is located just between the head group region and the hydrophobic core. Now, both the hydrocarbon segments and the hydroxyl groups have relatively more unfavorable contacts and the ring orientation is perpendicular to the direction of most molecules in the membrane. This all leads to a lower partition coefficient K than for the other two isomers mentioned above.

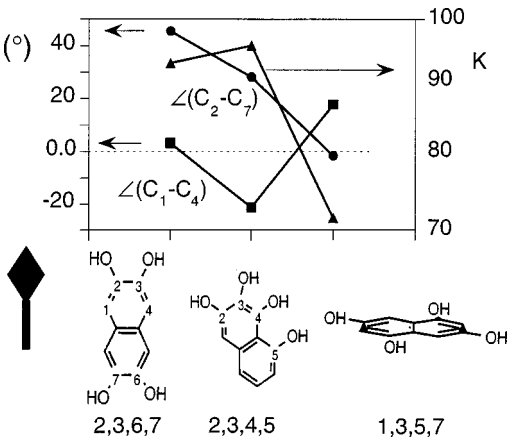

FIG. 10. The partition coefficients and the average orientation of the rings of 2,3,6,7,-tetrahydroxy naphthalene, 2,3,4,5-tetrahydroxy naphthalene, and 1,3,5,7-tetrahydroxy naphthalene in a DMPC membrane. The average orientation is described by the two angles that the two molecular vectors make with the plane of the membrane. One vector pointing from unit 4 to 1 of the ring $[\angle(C_1-C_4)]$ and the other pointing from unit 7 to 2 $[\angle(C_2-C_7)]$ are given. The pictorials represent the approximate average orientation with respect to the membrane, as indicated by the director (cf. Fig. 5). The conditions are the same as in Fig. 7.

We note that, in spite of their considerable orientational changes, the differences in the partition coefficient between these molecules are still relatively small, in comparison with those of the zwitterionic isomers. Apparently, electrostatics dominate over nonelectrostatic effects like the contact energies and the anisotropic field. The segment potential profile of the hydrocarbon or hydroxyl groups is changing much more moderately than that of the charged segments. So the positions of these segment types have less influence of the partition coefficient. Electrostatics amplify the positional and orientational variability in these systems as with respect to K.

IV. FURTHER DISCUSSION AND PERSPECTIVES

With a limited and *a priori* parameter set it was shown to be possible to calculate with an extended self-consistent-anisotropic-field theory the partition coefficient of various alcohols to a surprisingly good match with experimental data. Although we did not account for all the molecular details yet, we have predicted noticeable differences in partition coefficients within a group of similar molecules (isomers). Therefore, these differences cannot be assigned to aspects that were not yet included in the modeling. For instance, the difference between CH_2 and CH_3 groups for the partitioning of 4-isopropyl phenol and 4-*n*-propyl phenol is of minor importance, since our prediction of this difference is essentially correct without incorporating any structural difference between these two groups of atoms. The conformational consequences of branching prevails over any chemical difference between the CH, CH_2, and CH_3 groups.

The theoretical results give specific detail on the cause of the difference in partition coefficient of related molecules. It is found that in the partitioning of zwitterionic isomers into DMPC bilayers the location of the positive charge in the membrane is of crucial importance for the magnitude of the partition coefficient. The actual position and orientation of rigid (benzene) rings can be influenced by the relative position and the nature of substituents. Of these, positive charges, positioned close to the ring in the molecule, have the stronger influence on the position and the orientation of the molecule in the membrane and on the partition coefficient. Negative charges exert their influence mainly on the partition coefficient but not so much on the orientation of mainly hydrophobic molecules. Their segment potential profile shows hardly any gradients between the positions of phosphate groups on both sides of the DMPC membrane, which is the region where these molecules accumulate. The segment potential profile for positive charges has a steep gradient on the edge of the hydrophobic core on the inside of the head group profile. Therefore, their position in this region does play a role.

Details concerning the positions and the orientations of the additives can give valuable information on the working mechanism of biologically active molecules like drugs or hormones. Information like this may help to design new molecules and to evolve existing ones to improve their performance.

In this paper we considered extremely low amounts of additives in the membrane. In practical cases, however, a high loading is of obvious importance. Increasing the additive concentration in the bilayer can give rise to many interesting effects, which await further investigation. Such additive interactions can also be handled with the present approach.

V. CONCLUSIONS

We have demonstrated that it is possible to investigate the incorporation of complex foreign molecules in DMPC membranes with a detailed self-consistent-field model. With a limited and *a priori* parameter set, we have successfully predicted the partition coefficient of a number of linear and branched alcohols. Our partition coefficient compares well with literature data. The strength of our model is that predictions can be made for the partitioning of even more complex additives, such as molecules that contain rigid structures. We have studied a number of such molecules. We find that rigid structures serve as amplifiers in bringing about variation in partition coefficient in a series of isomers. Frequently the rigid rings orient mainly parallel to the tails in the lipid membrane. Only for specially designed additives we found the orientation of the ring to be parallel with the membrane surface. In general, we have observed that positively charged units do not penetrate the hydrophobic region of the membrane as easily as do negatively charged units. This can be rationalized considering the electrostatic potential profile through the DMPC bilayer.

We have proven that it is possible to design isomeric molecules that have virtually the same partition coefficient in lipid bilayers but that differ greatly with respect to the position and orientation of the molecule in the membrane. The fact that these properties can be uncoupled is an interesting observation that in the future may help the design of new drugs.

Our model assumes that all molecules behave ideally in a homogeneous bulk phase. We therefore suggest that our calculations should be combined with experimental data for partitioning of additives in an octanol/water two-phase system or should be accompanied by, e.g., MD simulations of the molecule or a set of molecules in a homogeneous aqueous bulk phase.

ACKNOWLEDGMENTS

We thank Bayer A.G. in Leverkusen, Federal Republic of Germany, for making this work possible both by financial support and Van Lent at Bayer AG, Leverkusen for providing us with some of the experimental data.

APPENDIX: GENERATION AND DEFINITION OF THE CONFORMATIONS q_{ki} OF A RIGID STRUCTURE

To describe conformers of a rigid structure, only three parameters are needed: the position of one of the segments and the direction of two independent vectors chosen from the coordinates of the segments in the structure. It is necessary that these two vectors can be chosen independently of the way the coordinates of all the segments are presented with respect to each other.

It is also important that the full set of all possible conformations of a rigid structure is reduced similarly to that of flexible chains on a lattice: a finite set of conformations must be generated. The number of allowed conformations should be comparable to that which two connected segments in a flexible chain can have. In this way, the number of degrees of freedom of a rigid structure is the same as that of two segments connected by a bond, which is, in essence, the smallest rigid structure. We chose here to use a simple cubic geometry to generate these conformations. In such a lattice it is logical to take six orientations per segment position. These orientations can be described simply by two independent vectors. We refer to those as $\mathbf{R}_{s_k}$ and $\mathbf{R}_{s_k\perp}$, the last one being perpendicular to the first one. The six conformations are defined as follows: conformation (1), with $\mathbf{R}_{s_k}$ in the z^+ direction, conformation (2), with $\mathbf{R}_{s_k\perp}$ in the z^+ direction, and conformation (3), with the outer product $\mathbf{R}_{s_k}\times\mathbf{R}_{s_k\perp}$ in the z^+ direction. The three other conformations are corresponding conformations parallel to the z^- direction. In Fig. 11 this procedure is visualized for a benzenelike molecule.

In the following we will first discuss how we determine the two determining vectors $\mathbf{R}_{s_k}$ and $\mathbf{R}_{s_k\perp}$ for an arbitrary rigid structure. The most descriptive vector for any (more or less flat) structure is the normal vector $\mathbf{N}_k$ of an average plane through the coordinates $\{\mathbf{r}_{s_k}\}$ of the segments that make up the structure. So, first this vector is calculated with the least square method according to Van Rootselaar.[43] To find the vector that describes the longest dimension of the structure, seen from the segment s_k, the position that code-

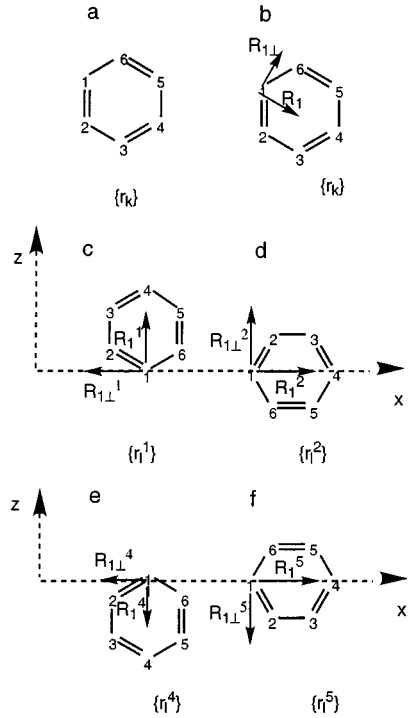

FIG. 11. Part (a) shows the structure of a six-membered ring (e.g., benzene). Part (b) shows the molecule with the main vector attached to segment 1 (R_1) and its outer product with the normal of the pane of the molecule ($R_{1\perp}$). Parts (c)–(f) show four of the six generated configurations with segment 1 as the segment in the origin. Only the conformations in the $x-y$ plane are given. Configurations 3 and 6 are not shown since these would be represented by a line (all six segments lay in the $x-y$ plane).

termines the conformation, first all coordinates $\{\mathbf{r}_{s_k})\}$ are translated over the vector of segment s_k ($\mathbf{r}_{s_k}$), $\mathfrak{T}\mathbf{r}_{s_k}$, so that segment s is in the origin:

$$\{\mathbf{r}_{s_k}\} \xrightarrow{\mathfrak{T}\mathbf{r}_{s_k}} \{\mathbf{r}'_{s_k}\}. \tag{A1}$$

The normalized sum of all the positional vectors is the vector that describes the longest dimension of the structure seen from the segment, s:

$$\mathbf{R}'_{s_k} = \frac{\Sigma_{s'_k}\mathbf{r}_{s'_k}}{|\Sigma_{s'_k}\mathbf{r}_{s'_k}|}, \tag{A2}$$

where the sum over s'_k runs over all the segments in the structure. To find the second independent vector to describe the orientations orthogonal to this vector, simply the normalized outer product of this vector, $\mathbf{R}_{s_k}$, with the normal of the structure is taken:

$$\mathbf{R}'_{s_{k\perp}} = \frac{\mathbf{R}'_{s_k}\times\mathbf{N}_k}{|\mathbf{R}'_{s_k}\times\mathbf{N}_k|}. \tag{A3}$$

With these two vectors the orientation of the structure is determined uniquely with respect to segment s in the origin. To determine the six orientations in the simple cubic lattice the following procedure is followed.

The translated coordinates are rotated so that $\mathbf{R}^1_{s_k}\|\mathbf{e}_z$ and $\mathbf{R}^1_{s_{k\perp}}\|\mathbf{e}_x$. Where $\mathbf{e}_x$, $\mathbf{e}_y$, and $\mathbf{e}_z$ are the base vectors and $\mathfrak{R}\mathbf{e}_z,\angle(\mathbf{R}'_{s_k},\mathbf{e}_x)$ is a rotation around vector $\mathbf{e}_z$) over the angle between $\mathbf{R}'_{s_k}$ and $\mathbf{e}_x(\angle(\mathbf{R}'_{s_k},\mathbf{e}_x))$:

$$\{\mathbf{r}'_{s_k},\mathbf{R}'_{s_k},\mathbf{R}'_{s_{k\perp}}\} \xrightarrow{\mathfrak{R}\mathbf{e}_z,\angle(\mathbf{R}'_{s_k},\mathbf{e}_x),\mathfrak{R}\mathbf{e}_y,\angle(\mathbf{R}'_{s_k},\mathbf{e}_z)} \{\mathbf{r}^1_{s_k},\mathbf{R}^1_{s_k},\mathbf{R}^1_{s_{k\perp}}\}. \tag{A4}$$

The coordinates $\mathbf{r}^1_{s_k}$ obtained in this way are determining the first configuration. The second configuration is obtained by pivoting around the y axis so that $\mathbf{R}^2_{s_k}\|\mathbf{e}_x$ and $\mathbf{R}^2_{s_{k\perp}}\|\mathbf{e}_z$:

$$\{\mathbf{r}^1_{s_k},\mathbf{R}^1_{s_k},\mathbf{R}^1_{s_{k\perp}}\} \xrightarrow{\mathfrak{R}\mathbf{e}_z,\angle(\mathbf{R}^1_{s_{k\perp}},\mathbf{e}_x),\mathfrak{R}\mathbf{e}_y,\angle\left(\frac{\pi}{2}\right)} \{\mathbf{r}^2_{s_k},\mathbf{R}^2_{k},\mathbf{R}^2_{k\perp}\}. \tag{A5}$$

The third configuration is generated by rotation around the x axis over $\pi/2$:

$$\{\mathbf{r}^2_{s_k},\mathbf{R}^2_{s_k},\mathbf{R}^2_{s_{k\perp}}\} \xrightarrow{\mathfrak{R}\mathbf{e}_x,\angle\left(\frac{\pi}{2}\right)} \{\mathbf{r}^3_{s_k},\mathbf{R}^3_{s_k},\mathbf{R}^3_{s_{k\perp}}\}. \tag{A6}$$

The configurations 4–6 are found by rotation of the configurations 1–3, respectively, around the x axis over an angle π:

$$\begin{aligned}
&\{\mathbf{r}^1_{s_k},\mathbf{R}^1_{s_k},\mathbf{R}^1_{s_{k\perp}}\} \xrightarrow{R\mathbf{e}_x,\angle(\pi)} \{\mathbf{r}^4_{s_k},\mathbf{R}^4_{s_k},\mathbf{R}^4_{s_{k\perp}}\},\\
&\{\mathbf{r}^2_{s_k},\mathbf{R}^2_{s_k},\mathbf{R}^2_{s_{k\perp}}\} \xrightarrow{\mathfrak{R}\mathbf{e}_x,\angle(\pi)} \{\mathbf{r}^5_{s_k},\mathbf{R}^5_{s_k},\mathbf{R}^5_{s_{k\perp}}\},\\
&\{\mathbf{r}^3_{s_k},\mathbf{R}^3_{s_k},\mathbf{R}^3_{s_{k\perp}}\} \xrightarrow{\mathfrak{R}\mathbf{e}_x,\angle(\pi)} \{\mathbf{r}^6_{s_k},\mathbf{R}^6_{s_k},\mathbf{R}^6_{s_{k\perp}}\}.
\end{aligned} \tag{A7}$$

The procedure given by Eqs. (A1)–(A7) is done for each segment in the structure. In this way the number of generated conformations of a structure, $N_{q_{ki}}=6N_{ki}M$, where N_{ki} is the number of units in structure k of molecule i. Every segment in the structure is the center of six conformations per layer. So, the number of conformations with a segment s in layer z for rigid structure k, $q_{ki}(z,s)$, is six times the number of segments in the structure. For each conformation, only the z coordinates of the members of the ring are relevant because the $x-y$ information is typically averaged out in a mean field theory.

1. The chemical potential

The chemical potential as given by Leermakers *et al.*[19] and calculated as the derivative with respect to the number of molecules of type i in the system of the canonical partition function for the homogeneous phase reads as

$$\begin{aligned}
\frac{\mu_i-\mu_i^*}{kT} = \ln\varphi_i^b - \frac{N_i}{2}\sum_A\sum_B(\varphi^*_{Ai}-\varphi^b_A)\chi_{AB}(\varphi^*_{Bi}-\varphi^b_B)\\
-\sum_{\alpha''}[(N_i-N_i^{\alpha''b})\ln(1-\varphi^{\alpha''b})-(N_i-N_i^{\alpha''*})\\
\times\ln(1-\varphi_i^{\alpha''*})].
\end{aligned} \tag{A8}$$

The last term in this equation can be rewritten by realizing that, when a phase is homogeneous, the volume fraction of bonds in a certain direction α'', $\varphi^{\alpha''b}$, and $\varphi^{\alpha''*}$, are equal to the sum over all the bonds divided by the number of directions Z:

$$\varphi^{\alpha''b}=\frac{1}{Z}\sum_j \frac{N_{\sigma j}}{N_j}\varphi_j^b \quad \text{and} \quad \varphi^{\alpha''*}=\frac{N_{\sigma i}}{ZN_i}\varphi_i^*. \tag{A9}$$

In this way the arguments of the logarithms are independent of α'' and can be taken through the summation. The sum over all direction of bonds of a molecule in the bulk, $N_i^{\alpha''b}$, is equal to all the bonds in the molecule, $N_{\sigma i}$. This also applies to $N_i^{\alpha''}*$. We now can execute the last summation of Eq. (A8), leading to

$$\sum_{\alpha''}\left[(N_i-N_i^{\alpha''b})\ln(1-\varphi^{\alpha''b})-(N_i-N_i^{\alpha''*})\ln(1-\varphi_i^{\alpha''*})\right]$$

$$=(ZN_i-N_{\sigma i})\ln\left[1+\frac{N_{\sigma i}-N_i\Sigma_j\dfrac{N_{\sigma j}\varphi_j^b}{N_j}}{ZN_i-N_{\sigma i}}\right], \tag{A10}$$

which directly leads to the formula given in the main text for the chemical potentials, Eq. (6).

For systems that are composed of molecules without ring structures, so that it contains only linear and branched chains, the number of bonds, $N_{\sigma i}$, is N_i-1. In this case Eq. (6) reduces to the result given in Ref. 42. For large Z the approximation $\ln(1+x)\approx x$ can be applied and Eq. (6) reduces to the usual Flory Huggins expression for μ_i:

$$\frac{\mu_i-\mu_i^*}{kT}=\ln\varphi_i^b-\frac{N_i}{2}\sum_A\sum_B(\varphi_{Ai}^*-\varphi_A^b)$$

$$\times\chi_{AB}(\varphi_{Bi}^*-\varphi_B^b)+1-N_i\sum_j\frac{\varphi_j^b}{N_j}. \tag{A11}$$

[1] J. S. Singer and G. L. Nicholson, Science **175**, 720–731 (1972).
[2] P. Yeagle, in *The Structure of Biological Membranes* (CRC Press, Boca Raton, 1992).
[3] P. van der Ploeg and H. J. C. Berendsen, J. Chem. Phys. **76**, 3271–3276 (1982).
[4] P. van der Ploeg and H. J. C. Berendsen, Mol. Phys. **49**, 233–248 (1983).
[5] H. J. C. Berendsen, B. Egberts, S.-J. Marrink, and P. Ahlström, in *Membrane Proteins: Structures, Interactions and Models*, edited by A. Pullman (Kluwer Academic, Dordrecht, 1992), pp. 457–470.
[6] E. Egberts and H. J. C. Berendsen, J. Chem. Phys. **89**, 3718–3732 (1988).
[7] M. M. Sperotto and O. G. Mouritsen, Eur. Biophys. J. **19**, 157–168 (1991).
[8] O. G. Mouritsen, K. Jorgensen, J. H. Ipsen, M. J. Zuckermann, and L. Cruzeiro-Hansson, Phys. Scr. **T33**, 42–51 (1990).
[9] J. H. Ipsen, K. Jorgensen, and O. G. Mouritsen, Biophys. J. **58**, 1099–1107 (1990).
[10] J. A. Marqusee and K. A. Dill, J. Chem. Phys. **85**, 434–444 (1986).
[11] D. W. R. Gruen, J. Phys. Chem. **89**, 146 (1985).
[12] D. W. R. Gruen and E. H. B. de Lacey, in *Surfactants in Solution*, edited by K. L. Mittal and B. Lindman (Plenum, New York, 1984), pp. 279–306.
[13] I. Szleifer, A. Ben-Shaul, and W. M. Gelbart, J. Chem. Phys. **83**, 3612–3620 (1985).
[14] A. Ben-Shaul, I. Szleifer, and W. M. Gelbart, J. Chem. Phys. **83**, 3597–3611 (1985).
[15] D. W. R. Gruen and D. A. Haydon, Pure Appl. Chem. **52**, 1229–1240 (1980).
[16] S. Marcelja, Biochim. Biophys. Acta **367**, 165–176 (1974).
[17] F. A. M. Leermakers and J. M. H. M. Scheutjens, J. Chem. Phys. **89**, 3264–3274 (1988).
[18] F. A. M. Leermakers and J. M. H. M. Scheutjens, J. Phys. Chem. **93**, 7417–7426 (1989).
[19] F. A. M. Leermakers and J. M. H. M. Scheutjens, J. Chem. Phys. **89**, 6912–6924 (1988).
[20] L. A. Meijer, F. A. M. Leermakers, and A. Nelson, Langmuir **10**, 1199–1206 (1994).
[21] A. Nelson, J. Chem. Soc., Faraday Trans. **89**, 2799–2805 (1993).
[22] A. Nelson, J. Chem. Soc., Faraday Trans. **89**, 3081–3090 (1993).
[23] L. A. Meijer, F. A. M. Leermakers, and J. Lyklema, Recl. Trav. Chim. Pays-Bas. **113**, 167–175 (1994).
[24] H. Hauser, I. Pasher, R. H. Pearson, and S. Sundell, Biochim. Biiophys. Acta **650**, 21–51 (1981).
[25] M. Björling, Ph.D. thesis, University of Lund, Sweden, 1992.
[26] P. A. Barneveld, D. E. Hesselink, F. A. M. Leermakers, J. Lyklema, and J. M. H. M. Scheutjens, Langmuir **10**, 1084–1092 (1994).
[27] M. R. Böhmer, O. A. Evers, and J. M. H. M. Scheutjens, Macromolecules **23**, 2288–2301 (1990).
[28] E. A. DiMarzio, J. Chem. Phys. **66**, 1160 (1977).
[29] E. A. DiMarzio, J. Chem. Phys. **35**, 658 (1961).
[30] O. A. Evers, J. M. H. M. Scheutjens, and G. J. Fleer, Macromolecules **23**, 5221–5233 (1990).
[31] T. L. Hill, *Thermodynamics of Small Systems* (Benjamin, New York, 1963, 1964), Vol. 1 and 2.
[32] D. G. Hall and B. A. Pethica, in *Nonionic Surfactants*, edited by M. J. Schick (Marcel Dekker, New York, 1976).
[33] P.-G. De Gennes and C. Taupin, J. Phys. Chem. **86**, 2294–2304 (1982).
[34] R. P. Rand and V. A. Parsegian, in *The Structure of Biological Membranes*, edited by P. Yeagle (CRC Press, Boca Raton, 1992), pp. 251–306.
[35] W. Helfrich, Naturforsch. **33a**, 305–315 (1978).
[36] C. Tanford, *The Hydrophobic Effect: Formation of Micelles and Biological Membranes* (Wiley, New York, 1973).
[37] S.-F. Tocanne and J. Teissié, Biochim. Biophys. Acta **1031**, 111–142 (1990).
[38] M. Gutman and E. Nachliel, Biochim. Biophys. Acta **1015**, 391–414 (1990).
[39] M. K. Granfeldt and S. J. Miklavic, J. Phys. Chem. **95**, 6351–6360 (1991).
[40] D. Stigter and K. A. Dill, Langmuir **4**, 200–209 (1988).
[41] S. S. Davis, M. J. James, and N. H. Anderson, Faraday Discuss. Chem. Soc. **81**, 1–15 (1986).
[42] L. A. Meijer, F. A. M. Leermakers, and J. Lyklema, J. Phys. Chem. **99**, 17 282–17 293 (1995).
[43] B. Van Rootselaar, *Lineaire Algebra* [Wolters-Noordhoff N.V., Groningen (NL), 1971].